GEORGIA INSTITUTE OF TECHNOLOGY

The George W. Woodruff School of Mechanical Engineering

Health Physics

Ph.D. Qualifiers Exam

Fall Semester, 1999

Day 1

Instructions

1. Complete 4 of the 6 questions.
2. Use a separate page for each answer sheet (no front to back answers).
3. The question number should be shown on each answer sheet.
4. Staple your question sheet to your answer sheets and turn in.

1. A NaI(Tl) detector is used to measure the activity of a ^{137}Cs source (refer to figure below for the decay scheme.

   Given:
   a. the absolute photopeak (i.e. the 0.662 MeV gamma photon) detection efficiency is 20%,
   b. the gross count associated with the photopeak is measured to be 1000 counts in 10 minutes, and
   c. the background count rate in the peak region is determined to be 10 ± 1 counts/min.

   Estimate the activity (in Bq) of the ^{137}Cs source. (Note: you must include the uncertainty in your result.)

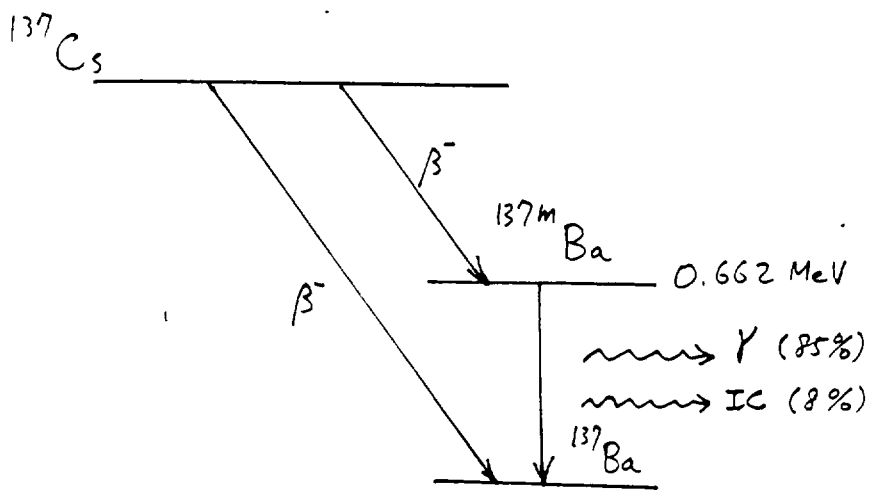

2. Discuss the direct action and indirect action as it pertains to radiation interactions in biological systems. Include in your discussions specific interactions, if pertinent, such as Compton scattering, the photoelectric effect, and pair-production.

3. You have just received from a vendor a 1-in dia. spherical ^{3}He-filled proportional counter. You are to verify the gas pressure inside the counter by placing it in an isotropic thermal neutron field with a known fluence rate of $\phi_{th} = 10^2$ n cm^{-2} s^{-1}. If the measured neutron count rate is 200 ± 0 cps, estimate the ^{3}He gas pressure (in atm) inside the counter.

   Data: the microscopic thermal neutron absorption cross section for ^{3}He(n,p)^{3}H is 5400 barns.

4. NASA's Voyager spacecraft, on a mission to Mars, was reported as "lost in space." Actually, the mission was reprogrammed by a group of Georgia Tech graduate students to land on Mars and search the terrestrial environment for candidate scintillation materials that display characteristics more nearly ideal than those materials found here on Earth. Early findings have turned up one promising candidate that has been colloquially named "Buzzite." The scintillation characteristics have been made available to you such that you can evaluate Buzzite for use back home on Earth. In addition to having Z_{eff}=90 and ρ=18 g/cm^3, Buzzite has a single scintillation decay time of τ=200 ps, an emission spectrum that peaks at 520 nm and a scintillation yield of 200,000 photons/MeV.

NaI(Tl) scintillation characteristics: $Z_{eff}\approx 52$, ρ=3.67 g/cm^3, τ=230 ns, peak emission wavelength = 415 nm, scintillation yield = 35,000 photons/MeV.

a. If NaI(Tl) and Bearcatite crystals of the same size and shape were placed in identical geometries with a ^{137}Cs source and identical photomultiplier tubes, calculate the limiting energy resolution for each of the two detectors due to photoelectron statistics. Assume a light collection efficiency of 85% for both detectors, a quantum efficiency of 30% for the NaI(Tl) detector, and a quantum efficiency of 20% for the Bearcatite detector.

b. Using the same scales for both axes, sketch the uncalibrated MCA pulse height spectrum that you would expect to record with the NaI(Tl) and Buzzite detectors described in Part a). Assume that identical high voltage, amplifier, and MCA settings are used for both scintillators.

(See attached chart.)

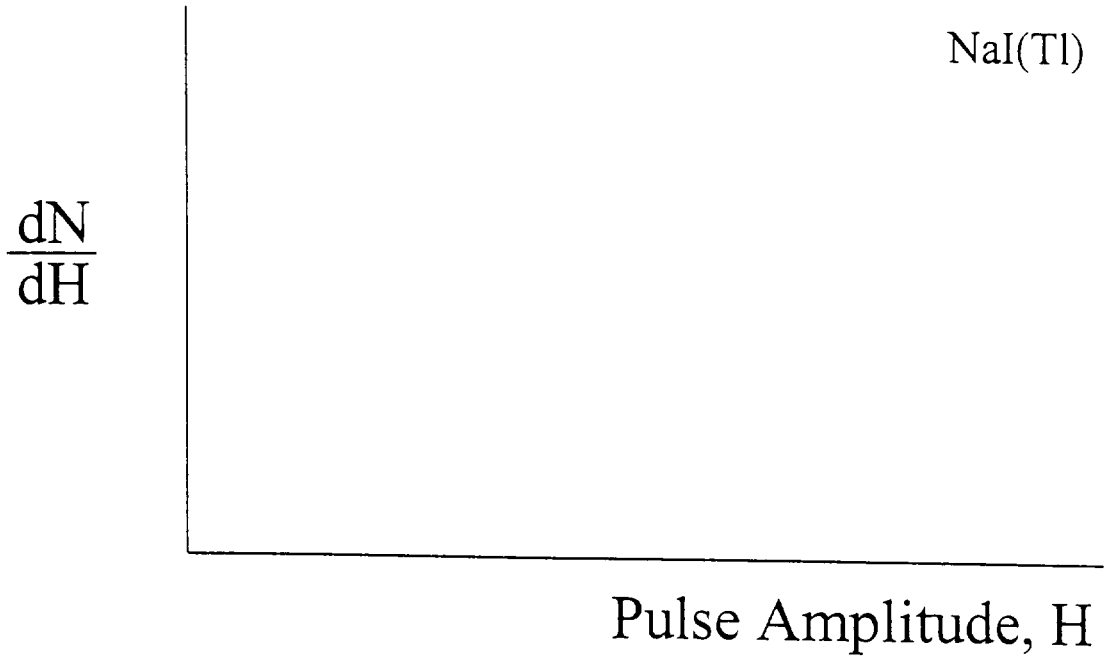
NaI(Tl)
dN/dH
Pulse Amplitude, H

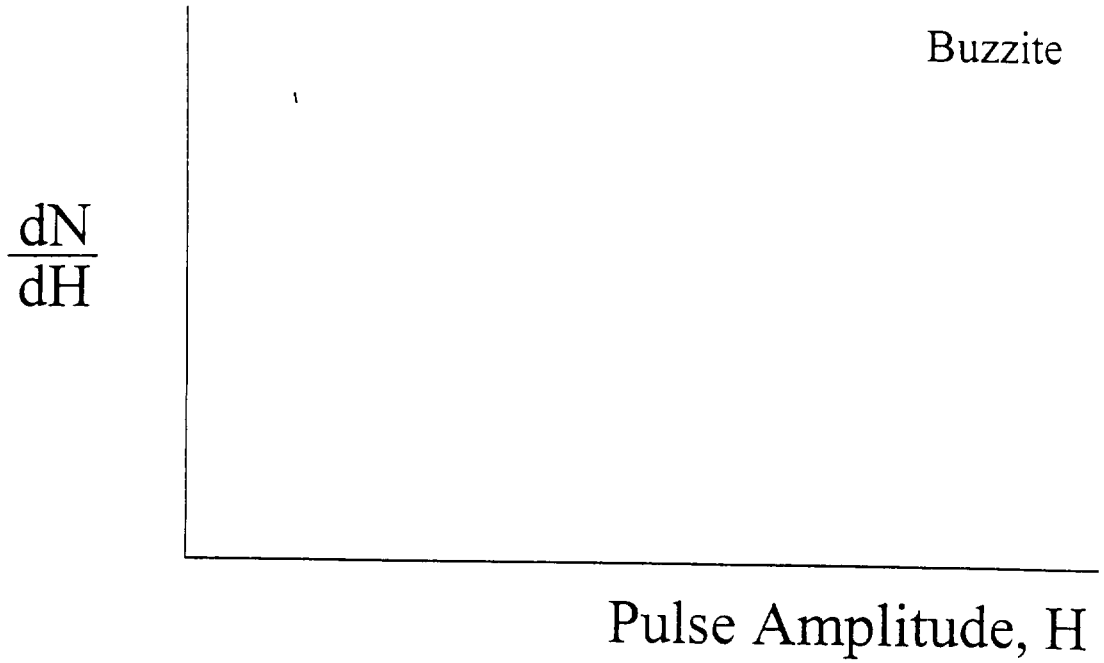
Buzzite
dN/dH
Pulse Amplitude, H

5. Unscheduled DNA repair as well as scheduled DNA repair can be prone to errors during the repair process. Discuss the intracellular processes used to ensure the repair processes are carried out with a high degree of reliability.

6. The "Semi-empirical Mass Equation" (or liquid drop model) can be used to obtain the expected mass and/or the binding energy of a nuclide.

   In symbolic form, show this equation for the expected **atomic mass** of a nuclide, **M**, with atomic number **Z**, and the mass number **A**.

   Briefly describe the source of each term in the binding energy portion of the equation.

GEORGIA INSTITUTE OF TECHNOLOGY

The George W. Woodruff School of Mechanical Engineering

Health Physics

Ph.D. Qualifiers Exam

Fall Semester, 1999

Day 2

Instructions

1. Complete 4 of the 6 questions.
2. Use a separate page for each answer sheet (no front to back answers).
3. The question number should be shown on each answer sheet.
4. Staple your question sheet to your answer sheets and turn in.

1. 10,000 Bq U-238 (half-life 4.47 E09y) decays to Th-234 (half-life 24.0d), which has been separated from U-238 at day zero.

   a. Calculate the mass of U-238, in g.

   b. Calculate the decay rate of Th-234 in Bq after 12.0 d.

   c. Briefly discuss the 3 types of radioactive parent-progeny relations and indicate which pertains to U-238 – Th-234.

2. A criticality accident occurs with a fissile material dissolved in a liquid. An instantaneous burst of 10^{19} fissions occurs, followed by a sustained criticality event which averages $2(10^{14})$ fissions per second. The sustained portion of the event lasts for 10 hours. The lumped fission product activity from 10 seconds to 1000 hours after a fission is

$$3.81(10^{-6})\, t^{-1.2}\ Bq/fission.$$

Where t is in days. At the end of the criticality event, the tank ruptures and empties the radioactive fission-product solution on the floor of a 10 m x 10 m room. The solution uniformly covers the entire floor.

a. What is the fission product activity in the solution 1 minute after the tank ruptures?

b. Assume every disintegration of a fission product nuclide emits one monoenergetic photon of 1 MeV, what is the gamma ray exposure at 1 m above the floor in that room one day after the tank ruptures? (Attack the problem as though you are the health physicist on duty at the station, i.e. you want the **best** answer you can get with **limited** resources and time).

(Attach chart)

3. a. Calculate the radiation dose rate in Gy/h, in air at a distance of 6 m from a 10 MBq point source of a radionuclide that emits one 1.2 – MeV gamma ray per disintegration. The mass energy absorption coefficient in air at that energy is 0.0271 cm^2g^{-1}.

   b. Calculate the radiation exposure rate in air, in X units per hour, under these conditions.

   c. Define:
      1. radiation dose rate
      2. radiation exposure rate
      3. Kerma

4. The Georgia Tech Research Reactor containment building is roughly 82 ft. in diameter (inner) and 50 feet tall. 600 mCi of Kr-85 ($T_{½}$ = 10.8 years) are released in the containment building. When the containment building was leak tested, ½% of its volume leaked in a 24-hour period.

   a. After the release, the containment building is not opened for 7 days, what is the concentration of Kr-85 in Bq/m^3 in the containment building at this time?

   b. A demolition worker is in the containment building for 10 hours a day for 3 days after the containment building is opened. What is the dose to her skin? (Assume the leakage rate does not change when she exits and enters the building.)

   For Kr-85, submersion DCF = $4.66(10^{-11})\frac{Sv\ m^3}{hr\ Bq}$

5. a. Briefly define and indicate the difference between:

   1. stochastic vs. deterministic radiation effects.
   2. acute vs. delayed effects of radiation on organisms.

   b. Briefly define and give the applications of:

   1. W_R, the radiation weighting factor
   2. W_T, the tissue weighting factor.

   c. Calculate the dose rate, in Gy/h, to an organ that weighs 3.50 g and contains 250,000 Bq of a radionuclide that emits beta particles of 0.090 MeV maximum energy and gamma rays of 2.0 MeV. One beta particle and one gamma ray are emitted per decay. The specific absorbed fraction for the gamma ray in the organ is 2.4 E-02 kg^{-1}.

6. A linear accelerator is used to bombard a tritium target with a 25-μA beam of 2.5 MeV protons, producing 1.2 MeV neutrons via the T (p,n) reaction. If the production rate is 1.8 (10^{-6}) neutrons/proton, the neutron removal cross section is 0.08 cm^{-1}, the DCF = 3.5 (10^{-8}) $\frac{rem-cm^3}{n}$.

   a. What is the dose equivalent 40 cm away from the target along the beam centerline?

   b. An operator is located 4 m from the target and shielded by a 50-cm thick concrete wall. What is his dose equivalent rate?

   c. Such a neutron field would have a fair amount of gamma-ray contamination. What kind of detection instrument would provide the best gamma discrimination while making a measurement of the neutron dose.

Table E.1. Gamma-ray buildup factors for air-kerma response to an isotropic point source in an infinite air medium. Also given is the total mass interaction coefficient used to calculate the mean-free-path length.

Mean free paths	Photon energy (MeV)										
	0.04	0.06	0.08	0.1	0.2	0.5	1	2	5	10	15
0	1.00	1.00	1.00	1.00	1.00	1.00	1.00	1.00	1.00	1.00	1.00
0.5	2.20	2.58	2.52	2.35	1.90	1.60	1.47	1.38	1.29	1.20	1.15
1	3.38	4.76	4.83	4.46	3.28	2.44	2.08	1.83	1.57	1.37	1.28
2	5.85	10.8	12.0	11.4	7.74	4.84	3.60	2.81	2.09	1.68	1.49
3	8.47	18.9	22.9	22.5	15.0	8.21	5.46	3.86	2.60	1.97	1.70
4	11.2	29.1	37.9	38.4	25.6	12.6	7.60	4.96	3.11	2.26	1.90
5	14.1	41.5	57.4	59.9	40.0	17.9	10.0	6.13	3.61	2.54	2.11
6	17.0	56.1	82	87.8	58.9	24.2	12.7	7.35	4.12	2.82	2.30
7	20.1	73.2	112	123	82.8	31.6	15.6	8.61	4.62	3.10	2.50
8	23.3	92.7	148	166	112	40.1	18.8	9.92	5.12	3.37	2.70
10	30.0	140	242	282	192	60.6	25.8	12.6	6.13	3.92	3.08
15	49.0	316	636	800	545	134	47.0	20.0	8.63	5.25	4.03
20	71.4	596	1350	1810	1220	241	72.8	27.9	11.1	6.55	4.96
25	97.2	1010	2540	3570	2360	385	103	36.2	13.6	7.84	5.87
30	126	1600	4390	6430	4150	567	136	45.0	16.1	9.11	6.75
35	159	2410	7140	10600	6770	788	173	54.0	18.5	10.4	7.58
40	195	3480	11100	15700	10500	1050	212	63.2	21.0	11.6	8.31
μ/ρ (cm^2/g)	0.2486	0.1875	0.1662	0.1541	0.1234	0.08172	0.06358	0.04447	0.02751	0.02045	0.01810

Source: Extracted from American National Standard ANSI/ANS-6.4.3-1991, published by the American Nuclear Society.

GEORGIA INSTITUTE OF TECHNOLOGY

The George W. Woodruff School of Mechanical Engineering

Health Physics

Ph.D. Qualifiers Exam

Fall Semester, 1999

Day 3

Instructions

1. Complete 4 of the 6 questions.
2. Use a separate page for each answer sheet (no front to back answers).
3. The question number should be shown on each answer sheet.
4. Staple your question sheet to your answer sheets and turn in.

(Some of the attachments can be used for more than one problem.)

1. What is the flux at the center (Point O) of a spherical shell source emitting S_o gamma rays per second? The shell's total attenuation and build-up properties for the gamma-rays can be described completely by an attenuation coefficient k, i.e. e^{-kt}.

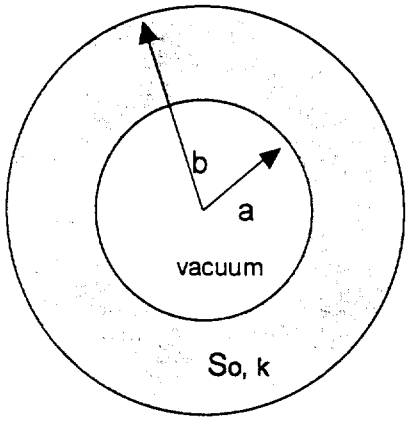

2. In a thyroid cancer treatment, ^{131}I is administered to the thyroid of a patient to deliver an average dose of 60 Gy. The following assumptions are made: (1) ^{131}I nuclides are uniformly distributed in the thyroid, (2) the thyroid is a perfect sphere of 2.5 cm in diameter, and (3) the biological half-life of iodine in thyroid is infinitely long. Refer to the attachment to:

   a. Estimate the activity of ^{131}I needed to be delivered to the thyroid, and
   b. Estimate the effective dose equivalent (H_E) incurred by the patient.

(See 12 pages of attachments.)

Table Weighting factors recommended by the Commission for stochastic risks

Organ or tissue	w_T
Gonads	0.25
Breast	0.15
Red bone marrow	0.12
Lung	0.12
Thyroid	0.03
Bone surfaces	0.03
Remainder	0.30

$$H_E = \sum_T w_T H_T$$

^{131}I 8.04 d

Radioactive Daughter		Half Life
^{131m}Xe	(1.1%)	11.84 d

Principal Beta Particles

Frequency (%)	Avg E (keV)	Max E (keV)
2.13	69.4	247.9
7.36	96.6	333.8
89.41	191.5	606.3
keV/decay	181.7	

Principal Conversion and Auger Electrons

Frequency (%)	Energy (keV)
3.63	45.6
1.55	329.9
keV/decay	10.1 *

Principal Gamma and X Rays

Frequency (%)	Energy (keV)
1.40	29.5
2.59	29.8
2.62	80.2
6.06	284.3
81.24	364.5
7.27	637.0
1.80	722.9
keV/decay	381.6

Table G–4 (cont'd) Fraction of photon energy released in source organ and absorbed in lungs, based on ICRP Publication 23.

Target: Lungs

Source	Photon energy (MeV)					
	0.010	0.015	0.020	0.030	0.050	0.100
Bladder	4.25E–26[a]	6.38E–26	5.54E–14	7.64E–08	1.31E–05	8.88E–05
Stomach	1.76E–04	2.64E–04	2.60E–03	7.90E–03	9.60E–03	6.91E–03
Small intestine	4.44E–15	6.66E–15	9.64E–09	6.30E–05	4.61E–04	7.92E–04
Upper large intestine	3.97E–15	5.94E–15	1.18E–08	7.15E–05	6.13E–04	9.95E–04
Lower large intestine	2.61E–14	3.92E–17	4.15E–10	2.91E–06	1.15E–04	2.87E–04
Kidneys	3.57E–05	5.35E–05	7.14E–05	1.18E–03	3.27E–03	3.37E–03
Liver	7.75E–05	3.19E–03	9.45E–03	1.64E–03	1.45E–02	9.91E–03
Lungs	8.16E–01	6.57E–01	4.71E–01	2.30E–01	8.98E–02	5.04E–02
Other tissue (muscle)	3.89E–03	6.81E–03	9.43E–03	9.99E–03	7.04E–03	4.87E–03
Ovaries	5.11E–23	7.67E–23	1.02E–11	9.25E–07	8.57E–05	2.06E–04
Pancreas	2.75E–06	4.12E–06	1.16E–03	8.86E–03	1.29E–02	1.02E–02
Skeleton	1.69E–04	2.54E–04	1.04E–03	3.20E–03	4.42E–03	3.63E–03
Skin	8.03E–05	1.21E–04	7.44E–04	2.54E–03	2.94E–03	2.17E–03
Spleen	6.49E–04	9.75E–04	4.97E–03	1.25E–02	1.23E–02	8.96E–03
Testes	2.24E–33	3.36E–33	1.83E–17	1.65E–09	1.49E–06	1.23E–05
Thyroid	1.52E–10	2.28E–09	3.30E–05	1.23E–03	3.89E–03	3.67E–03
Total body	1.32E–02	1.34E–02	1.43E–02	1.26E–02	8.39E–03	5.40E–03

Source	Photon energy (MeV)					
	0.200	0.500	1.000	1.500	2.000	4.000
Bladder	9.32E–05	1.65E–04	2.83E–04	3.07E–04	3.31E–04	4.61E–04
Stomach	5.96E–03	6.39E–03	5.71E–03	5.50E–03	4.91E–03	4.28E–03
Small intestine	9.01E–04	1.16E–03	1.17E–03	1.07E–03	1.17E–03	1.13E–03
Upper large intestine	9.82E–04	1.17E–03	1.38E–03	1.43E–03	1.28E–03	1.13E–03
Lower large intestine	3.14E–04	3.49E–04	5.48E–04	5.48E–04	7.80E–04	5.77E–04
Kidneys	2.99E–03	3.28E–03	3.30E–03	2.96E–03	2.80E–03	2.72E–03
Liver	8.83E–03	8.22E–03	7.89E–03	7.71E–03	6.95E–03	5.59E–03
Lungs	5.00E–02	5.00E–02	4.55E–02	4.32E–02	3.92E–02	3.08E–02
Other tissue (muscle)	4.61E–03	4.62E–03	4.31E–03	4.04E–03	3.81E–03	3.17E–03
Ovaries	2.56E–04	3.88E–04	5.39E–04	5.61E–04	5.85E–04	7.00E–04
Pancreas	8.91E–03	8.20E–03	7.42E–03	6.76E–03	6.53E–03	5.19E–03
Skeleton	3.50E–03	3.38E–03	3.29E–03	3.03E–03	3.09E–03	2.30E–03
Skin	2.27E–03	2.34E–03	2.37E–03	2.33E–03	2.23E–03	1.84E–03
Spleen	7.90E–03	7.55E–03	6.86E–03	6.20E–03	6.37E–03	5.22E–03
Testes	4.38E–05	4.94E–05	1.01E–04	1.60E–04	1.20E–04	1.68E–04
Thyroid	3.38E–03	3.67E–03	3.83E–03	3.35E–03	3.17E–03	3.22E–03
Total body	4.97E–03	5.35E–03	4.58E–03	4.05E–03	3.85E–03	3.45E–03

[a]Read as 4.25×10^{-26}.

Source: ICRP 1975.

Table G–4 (cont'd) Fraction of photon energy released in source organ and absorbed in liver, based on ICRP Publication 23.

Target: Liver

Source	Photon energy (MeV)					
	0.010	0.015	0.020	0.030	0.050	0.100
Bladder	4.72E–16[a]	7.08E–16	4.29E–09	3.71E–05	4.92E–04	1.00E–03
Stomach	3.87E–04	5.83E–04	7.76E–04	7.22E–03	1.50E–02	1.46E–02
Small intestine	1.38E–04	6.37E–04	2.41E–03	8.31E–03	1.39E–02	1.30E–02
Upper large intestine	2.86E–04	4.29E–04	3.49E–03	1.34E–02	2.14E–02	1.81E–02
Lower large intestine	5.29E–14	7.93E–14	4.24E–08	5.88E–05	8.33E–04	1.80E–03
Kidneys	8.02E–04	1.20E–03	8.47E–03	2.79E–02	3.53E–02	2.77E–02
Liver	9.70E–01	8.98E–01	7.86E–01	5.38E–01	2.75E–01	1.65E–01
Lungs	1.30E–04	4.13E–03	1.31E–02	2.53E–02	2.33E–02	1.72E–02
Other tissue (muscle)	1.11E–03	3.48E–03	6.43E–03	9.99E–03	9.50E–03	7.40E–03
Ovaries	1.90E–11	2.86E–11	1.04E–06	4.38E–04	2.43E–03	3.62E–03
Pancreas	2.79E–04	4.16E–04	6.53E–03	2.97E–02	4.05E–02	3.19E–02
Skeleton	2.24E–04	3.38E–04	8.67E–04	3.02E–03	4.29E–03	4.62E–03
Skin	8.63E–05	1.29E–04	8.80E–04	3.22E–03	4.20E–03	3.64E–03
Spleen	1.30E–09	1.95E–09	7.69E–06	1.08E–03	5.30E–03	6.84E–03
Testes	4.67E–23	7.00E–23	1.74E–12	4.96E–07	4.94E–05	1.75E–04
Thyroid	2.28E–21	3.44E–21	2.10E–11	2.15E–06	3.49E–04	5.52E–04
Total body	2.61E–02	2.57E–02	2.57E–02	2.23E–02	1.63E–02	1.13E–02

Source	Photon energy (MeV)					
	0.200	0.500	1.000	1.500	2.000	4.000
Bladder	1.39E–03	1.77E–03	1.85E–03	1.74E–03	2.15E–03	1.88E–03
Stomach	1.27E–02	1.27E–02	1.15E–02	1.11E–02	1.12E–02	8.85E–03
Small intestine	1.20E–02	1.12E–02	1.11E–02	1.03E–02	9.92E–03	7.95E–03
Upper large intestine	1.69E–02	1.53E–02	1.47E–02	1.39E–02	1.31E–02	1.14E–02
Lower large intestine	1.85E–03	2.15E–03	2.33E–03	2.72E–03	2.24E–03	2.14E–03
Kidneys	2.46E–02	2.50E–02	2.21E–02	2.08E–02	1.99E–02	1.59E–02
Liver	1.60E–01	1.60E–01	1.46E–01	1.35E–01	1.24E–01	1.01E–01
Lungs	1.59E–02	1.48E–02	1.40E–02	1.30E–02	1.18E–02	1.05E–02
Other tissue (muscle)	6.91E–03	6.97E–03	6.68E–03	6.26E–03	5.97E–03	5.07E–03
Ovaries	3.82E–03	3.82E–03	3.93E–03	3.87E–03	4.16E–03	3.19E–03
Pancreas	2.82E–02	2.55E–02	2.33E–02	2.19E–02	1.95E–02	1.72E–02
Skeleton	4.33E–03	4.42E–03	4.36E–03	4.16E–03	4.53E–03	3.71E–03
Skin	3.66E–03	4.24E–03	4.07E–03	3.98E–03	4.00E–03	3.13E–03
Spleen	6.64E–03	6.68E–03	6.39E–03	6.24E–03	5.92E–03	5.10E–03
Testes	2.68E–04	3.20E–04	6.53E–04	7.53E–04	7.37E–04	7.19E–04
Thyroid	7.75E–04	9.94E–04	1.18E–03	1.32E–03	1.59E–03	1.40E–03
Total body	1.05E–02	1.08E–02	1.07E–02	9.09E–03	8.58E–03	7.75E–03

[a]Read as 4.72×10^{-16}.

Source: ICRP 1975.

Table G-4 (cont'd) Fraction of photon energy released in source organ and absorbed in red marrow, based on ICRP Publication 23.

Target: Red Marrow

Source	Photon energy (MeV)					
	0.010	0.015	0.020	0.030	0.050	0.100
Bladder	4.26E-05[a]	6.38E-05	8.51E-05	5.82E-03	1.85E-02	1.50E-02
Stomach	6.00E-05	9.00E-05	1.00E-03	5.48E-03	1.28E-02	1.07E-02
Small intestine	1.36E-03	4.46E-03	1.11E-02	3.12E-02	4.59E-02	2.88E-02
Upper large intestine	1.04E-03	1.56E-03	8.60E-03	2.90E-02	3.93E-02	2.49E-02
Lower large intestine	2.72E-04	8.55E-03	3.56E-02	7.86E-02	7.02E-02	3.42E-02
Kidneys	8.99E-04	1.35E-03	8.58E-03	3.02E-02	4.14E-02	2.54E-02
Liver	9.05E-05	7.91E-04	2.94E-03	8.52E-03	1.40E-02	1.07E-02
Lungs	4.22E-05	1.13E-03	5.96E-03	1.80E-02	2.19E-02	1.25E-02
Other tissue (muscle)	3.02E-03	6.90E-03	1.31E-02	2.39E-02	2.34E-02	1.32E-02
Ovaries	1.71E-04	2.57E-04	8.78E-03	4.92E-02	6.77E-02	3.75E-02
Pancreas	1.18E-04	1.77E-04	2.19E-03	1.37E-02	2.67E-02	1.91E-02
Skeleton	1.41E-01	1.33E-01	1.25E-01	9.68E-02	5.66E-02	2.48E-02
Skin	2.42E-03	5.85E-03	8.96E-03	1.20E-02	1.11E-02	6.03E-03
Spleen	1.06E-05	4.53E-04	2.61E-03	9.11E-03	1.58E-02	1.12E-02
Testes	4.86E-06	7.29E-06	9.74E-06	9.69E-04	4.83E-03	4.68E-03
Thyroid	4.02E-06	6.03E-06	4.71E-04	4.11E-03	9.69E-03	7.31E-03
Total body	2.34E-02	2.54E-02	2.93E-02	3.44E-02	2.85E-02	1.52E-02

Source	Photon energy (MeV)					
	0.200	0.500	1.000	1.500	2.000	4.000
Bladder	9.15E-03	6.50E-03	5.58E-03	5.21E-03	5.04E-03	4.61E-03
Stomach	6.96E-03	5.42E-03	4.77E-03	4.35E-03	4.17E-03	3.99E-03
Small intestine	1.74E-02	1.29E-02	1.17E-02	1.06E-02	1.02E-02	8.28E-03
Upper large intestine	1.49E-02	1.12E-02	9.60E-03	9.08E-03	8.79E-03	7.28E-03
Lower large intestine	2.04E-02	1.61E-02	1.45E-02	1.32E-02	1.27E-02	1.02E-02
Kidneys	1.58E-02	1.29E-02	1.17E-02	1.11E-02	1.02E-02	8.78E-03
Liver	6.96E-03	5.58E-03	4.82E-03	4.89E-03	4.76E-03	3.93E-03
Lungs	7.82E-03	6.53E-03	6.03E-03	5.54E-03	5.55E-03	4.53E-03
Other tissue (muscle)	8.37E-03	7.13E-03	6.39E-03	5.78E-03	5.93E-03	4.47E-03
Ovaries	2.15E-02	1.59E-02	1.40E-02	1.28E-02	1.21E-02	9.48E-03
Pancreas	1.16E-02	8.96E-03	8.01E-03	7.71E-03	7.14E-03	5.81E-03
Skeleton	1.73E-02	1.59E-02	1.52E-02	1.38E-02	1.26E-02	1.06E-02
Skin	4.28E-03	4.08E-03	3.95E-03	3.89E-03	3.48E-03	3.09E-03
Spleen	7.56E-03	5.85E-03	5.46E-03	5.03E-03	4.65E-03	4.23E-03
Testes	3.38E-03	2.72E-03	2.54E-03	2.27E-03	2.42E-03	2.12E-03
Thyroid	4.91E-03	4.34E-03	3.86E-03	3.84E-03	3.71E-03	3.17E-03
Total body	9.86E-03	8.52E-03	7.76E-03	7.07E-03	6.98E-03	5.46E-03

[a]Read as 4.26×10^{-5}.

Source: ICRP 1975.

Table G–4 (cont'd) Fraction of photon energy released in source organ and absorbed in stomach, based on ICRP Publication 23.

Target: Stomach

Source	Photon energy (MeV)					
	0.010	0.015	0.020	0.030	0.050	0.100
Bladder	4.25E–16[a]	6.38E–16	1.80E–09	4.92E–06	6.80E–05	1.58E–04
Stomach	4.82E–02	1.14E–01	1.34E–01	1.03E–01	4.92E–02	2.82E–02
Small intestine	8.54E–05	2.70E–04	1.23E–03	2.13E–03	2.66E–03	2.18E–03
Upper large intestine	3.17E–04	4.74E–04	1.71E–03	3.33E–03	3.08E–03	2.24E–03
Lower large intestine	1.88E–06	2.82E–06	1.29E–04	7.55E–04	1.20E–03	1.04E–03
Kidneys	2.03E–07	3.05E–07	8.18E–05	1.20E–03	2.39E–03	2.21E–03
Liver	5.78E–05	8.67E–05	1.16E–04	6.12E–04	1.34E–03	1.06E–03
Lungs	8.06E–05	1.21E–04	5.18E–04	1.21E–03	1.42E–03	1.08E–03
Other tissue (muscle)	5.97E–06	1.73E–04	5.88E–04	1.15E–03	1.10E–03	6.90E–04
Ovaries	1.21E–11	1.82E–11	3.11E–07	7.83E–05	3.60E–04	4.86E–04
Pancreas	3.39E–04	5.87E–03	1.65E–02	2.36E–02	1.70E–02	1.01E–02
Skeleton	2.17E–05	3.27E–05	4.35E–05	1.59E–04	2.60E–04	3.17E–04
Skin	4.11E–05	6.17E–05	8.22E–05	3.03E–04	3.87E–04	3.09E–04
Spleen	1.29E–04	1.94E–04	2.01E–03	8.00E–03	8.79E–03	6.14E–03
Testes	2.09E–23	3.12E–23	5.60E–13	9.99E–08	9.27E–06	1.29E–05
Thyroid	3.11E–23	4.67E–23	6.75E–13	1.09E–07	3.02E–05	2.85E–05
Total body	2.07E–03	2.12E–03	2.19E–03	1.71E–03	1.29E–03	8.64E–04

Source	Photon energy (MeV)					
	0.200	0.500	1.000	1.500	2.000	4.000
Bladder	1.53E–04	1.65E–04	2.79E–04	1.95E–04	2.75E–04	2.30E–04
Stomach	2.67E–02	2.69E–02	2.48E–02	2.22E–02	2.12E–02	1.73E–02
Small intestine	1.97E–03	1.74E–03	1.71E–03	1.62E–03	1.48E–03	1.18E–03
Upper large intestine	1.98E–03	1.86E–03	1.74E–03	1.42E–03	1.52E–03	1.16E–03
Lower large intestine	9.51E–04	9.35E–04	7.47E–04	7.10E–04	8.24E–04	7.38E–04
Kidneys	1.80E–03	1.74E–03	1.61E–03	1.27E–03	1.50E–03	1.22E–03
Liver	1.04E–03	9.75E–04	9.66E–04	9.00E–04	9.17E–04	7.76E–04
Lungs	9.92E–04	9.48E–04	9.51E–04	9.21E–04	9.68E–04	4.58E–04
Other tissue (muscle)	7.44E–04	7.26E–04	6.90E–04	6.57E–04	6.15E–04	5.18E–04
Ovaries	4.23E–04	4.35E–04	3.72E–04	4.88E–04	4.68E–04	4.70E–04
Pancreas	9.81E–03	8.76E–03	8.10E–03	7.44E–03	6.81E–03	6.03E–03
Skeleton	3.11E–04	3.03E–04	2.64E–04	2.85E–04	2.58E–04	2.22E–04
Skin	2.96E–04	3.36E–04	3.35E–04	3.06E–04	2.91E–04	2.42E–04
Spleen	5.04E–03	5.08E–03	4.40E–03	4.71E–03	3.98E–03	3.09E–03
Testes	2.57E–05	6.11E–05	4.07E–05	6.09E–05	7.20E–05	6.78E–05
Thyroid	2.17E–05	6.66E–05	6.93E–05	9.63E–05	5.55E–05	7.80E–05
Total body	1.01E–03	9.21E–04	8.22E–04	6.14E–04	6.90E–04	5.97E–04

[a]Read as 4.25×10^{-16}.

Source: ICRP 1975.

Table G–4 (cont'd) Fraction of photon energy released in source organ and absorbed in kidneys, based on ICRP Publication 23.

Target: Kidneys

Source	Photon energy (MeV)					
	0.010	0.015	0.020	0.030	0.050	0.100
Bladder	4.32E–17[a]	6.48E–17	1.12E–09	6.99E–06	1.15E–04	2.83E–04
Stomach	1.09E–07	1.63E–07	1.18E–04	2.32E–03	4.69E–03	3.86E–03
Small intestine	1.40E–06	2.10E–06	2.39E–04	1.97E–03	3.64E–03	3.69E–03
Upper large intestine	9.03E–08	1.35E–07	1.01E–04	1.64E–03	3.55E–03	3.24E–03
Lower large intestine	1.20E–09	1.81E–09	3.72E–06	2.53E–04	7.36E–04	8.86E–04
Kidneys	9.32E–01	7.78E–01	5.79E–01	2.93E–01	1.12E–01	6.67E–02
Liver	2.38E–04	3.58E–04	1.28E–03	4.46E–03	5.54E–03	4.49E–03
Lungs	1.82E–08	2.74E–08	1.65E–05	3.52E–04	8.43E–04	9.23E–04
Other tissue (muscle)	4.03E–04	1.26E–03	2.10E–03	2.50E–03	1.93E–03	1.45E–03
Ovaries	1.05E–11	1.58E–11	5.40E–07	1.55E–04	7.50E–04	1.00E–03
Pancreas	6.42E–06	9.63E–06	9.17E–04	7.10E–03	9.57E–03	7.53E–03
Skeleton	8.58E–05	1.29E–04	1.72E–04	5.14E–04	9.26E–04	8.55E–04
Skin	5.17E–05	7.72E–05	3.35E–04	7.98E–04	8.26E–04	5.91E–04
Spleen	1.99E–03	2.98E–03	1.03E–02	1.89E–02	1.51E–02	1.03E–02
Testes	1.33E–24	1.99E–24	2.56E–13	1.23E–07	1.08E–05	3.29E–05
Thyroid	2.52E–27	3.78E–27	1.13E–14	2.64E–08	5.85E–06	3.41E–05
Total body	3.98E–03	4.12E–03	3.64E–03	3.01E–03	2.33E–03	1.70E–03

Source	Photon energy (MeV)					
	0.200	0.500	1.000	1.500	2.000	4.000
Bladder	2.84E–04	3.78E–04	3.32E–04	4.80E–04	3.58E–04	3.89E–04
Stomach	3.58E–03	3.21E–03	3.01E–03	2.79E–03	2.55E–03	2.11E–03
Small intestine	3.07E–03	3.10E–03	2.93E–03	2.46E–03	2.44E–03	1.78E–03
Upper large intestine	2.79E–03	2.65E–03	2.67E–03	2.44E–03	2.08E–03	1.78E–03
Lower large intestine	9.85E–04	8.07E–04	8.75E–04	8.46E–04	1.01E–03	7.10E–04
Kidneys	6.79E–02	7.16E–02	6.42E–02	6.08E–02	5.48E–02	4.63E–02
Liver	3.86E–03	3.66E–03	3.35E–03	3.24E–03	3.12E–03	2.34E–03
Lungs	8.92E–04	1.03E–03	9.14E–04	1.03E–03	6.56E–04	8.01E–04
Other tissue (muscle)	1.41E–03	1.40E–03	1.34E–03	1.27E–03	1.20E–03	1.01E–03
Ovaries	9.85E–04	1.11E–03	1.03E–03	9.43E–04	1.03E–03	8.46E–04
Pancreas	6.45E–03	6.05E–03	5.51E–03	5.17E–03	4.63E–03	4.17E–03
Skeleton	9.34E–04	8.86E–04	1.14E–03	8.97E–04	6.90E–04	6.59E–04
Skin	6.50E–04	7.36E–04	7.38E–04	6.76E–04	6.53E–04	5.62E–04
Spleen	8.92E–03	8.32E–03	7.36E–03	7.24E–03	6.62E–03	5.08E–03
Testes	6.82E–05	9.97E–05	1.44E–04	1.60E–04	1.15E–04	2.06E–04
Thyroid	3.98E–05	4.80E–05	1.17E–04	1.69E–04	1.24E–04	8.78E–05
Total body	1.73E–03	1.72E–03	1.68E–03	1.39E–03	1.33E–03	1.12E–03

[a]Read as 4.32×10^{-17}.

Source: ICRP 1975.

Table G-4 (cont'd) Fraction of photon energy released in source organ and absorbed in testes, based on ICRP Publication 23.

Target: Testes

Source	Photon energy (MeV)					
	0.010	0.015	0.020	0.030	0.050	0.100
Bladder	6.64E-08[a]	9.98E-08	5.16E-05	5.71E-04	1.02E-03	6.97E-04
Stomach	1.27E-24	1.90E-24	7.01E-14	1.93E-08	2.04E-06	5.86E-06
Small intestine	1.02E-16	1.53E-16	6.23E-10	1.78E-06	1.81E-05	4.08E-05
Upper large intestine	4.56E-16	6.86E-16	9.46E-10	1.78E-06	1.88E-05	3.46E-05
Lower large intestine	1.73E-08	2.60E-08	8.20E-06	1.64E-04	3.19E-04	2.33E-04
Kidneys	1.63E-25	2.44E-25	3.16E-14	1.61E-08	1.95E-06	1.02E-05
Liver	8.05E-25	1.21E-24	3.48E-14	1.03E-08	1.27E-06	7.05E-06
Lungs	3.16E-34	4.75E-34	2.14E-18	2.06E-10	1.87E-07	7.12E-07
Other tissue (muscle)	1.85E-06	2.67E-05	9.87E-05	2.12E-04	2.05E-04	1.59E-04
Pancreas	3.58E-28	5.38E-28	1.81E-15	4.34E-09	9.28E-07	6.08E-06
Skeleton	6.72E-10	1.01E-09	8.24E-07	3.08E-05	6.42E-05	9.61E-05
Skin	3.07E-05	2.16E-04	3.19E-04	3.51E-04	1.80E-04	1.13E-04
Spleen	4.53E-28	6.79E-28	1.71E-15	3.61E-09	7.75E-07	5.27E-06
Testes	9.02E-01	6.90E-01	4.56E-01	1.98E-01	6.57E-02	3.97E-02
Thyroid	9.20E-27	1.38E-26	1.84E-26	2.72E-14	6.20E-10	2.92E-08
Total body	5.75E-04	4.71E-04	3.47E-04	3.30E-04	2.29E-04	1.62E-04

Source	Photon energy (MeV)					
	0.200	0.500	1.000	1.500	2.000	4.00
ladder	5.90E-04	6.49E-04	5.82E-04	4.75E-04	5.19E-04	4.49E-04
Stomach	8.94E-06	2.99E-06	2.12E-05	2.19E-05	2.21E-05	2.08E-05
Small intestine	4.75E-05	4.60E-05	6.64E-05	7.12E-05	7.87E-05	4.38E-05
Upper large intestine	4.27E-05	6.60E-05	7.12E-05	4.82E-05	6.46E-05	5.60E-05
Lower large intestine	2.69E-04	2.65E-04	1.80E-04	1.79E-04	2.26E-04	1.45E-04
Kidneys	1.57E-05	1.92E-05	2.14E-05	2.20E-05	2.22E-05	2.10E-05
Liver	1.13E-05	1.45E-05	3.25E-05	1.74E-05	1.78E-05	1.71E-05
Lungs	1.71E-06	3.13E-06	4.53E-06	5.31E-06	5.86E-06	6.46E-06
Other tissue (muscle)	1.54E-04	1.58E-04	1.51E-04	1.47E-04	1.70E-04	1.19E-04
Pancreas	1.02E-05	7.98E-06	1.59E-05	1.67E-05	1.71E-05	1.66E-05
Skeleton	8.27E-05	7.35E-05	8.31E-05	8.79E-05	1.44E-04	7.90E-05
Skin	1.42E-04	1.06E-04	1.15E-04	1.14E-04	1.10E-04	1.19E-04
Spleen	9.09E-06	1.22E-05	1.44E-05	1.54E-05	1.58E-05	1.55E-05
Testes	4.34E-02	4.56E-02	4.30E-02	3.86E-02	3.64E-02	2.84E-02
Thyroid	1.31E-07	4.34E-07	9.13E-07	1.30E-06	1.62E-06	2.23E-06
Total body	1.42E-04	2.41E-04	2.12E-04	1.82E-04	1.70E-04	1.60E-04

[a]Read as 6.64×10^{-8}.

Source: ICRP 1975.

Table G–4 (cont'd) Fraction of photon energy released in source organ and absorbed in ovaries, based on ICRP Publication 23.

Target: Ovaries

Source	Photon energy (MeV)					
	0.010	0.015	0.020	0.030	0.050	0.100
Bladder	5.15E–08[a]	7.73E–08	1.34E–05	2.30E–04	2.96E–04	2.33E–04
Stomach	1.65E–13	2.46E–13	8.68E–09	2.39E–06	1.95E–05	1.76E–05
Small intestine	1.14E–04	1.71E–04	3.66E–04	5.18E–04	5.38E–04	3.50E–04
Upper large intestine	1.66E–04	2.50E–04	4.41E–04	6.13E–04	4.62E–04	3.75E–04
Lower large intestine	3.39E–04	5.09E–04	1.34E–03	1.46E–03	8.77E–04	5.17E–04
Kidneys	3.04E–13	4.57E–13	1.46E–08	3.98E–06	3.07E–05	3.42E–05
Liver	8.12E–14	1.22E–13	4.59E–09	1.35E–06	1.25E–05	1.35E–05
Lungs	4.34E–23	6.52E–23	2.88E–13	2.59E–08	1.90E–06	2.50E–06
Other tissue (muscle)	3.40E–05	7.70E–05	9.84E–05	1.02E–04	8.27E–05	6.26E–05
Ovaries	8.01E–01	4.89E–01	2.70E–01	9.51E–02	2.96E–02	1.84E–02
Pancreas	4.37E–17	6.55E–17	2.54E–10	6.61E–07	1.07E–05	1.51E–05
Skeleton	1.75E–07	2.63E–07	7.47E–06	3.18E–05	2.65E–05	2.32E–05
Skin	7.12E–11	1.07E–10	1.60E–07	6.35E–06	1.54E–05	1.01E–05
Spleen	8.12E–16	1.22E–15	6.57E–10	7.28E–07	9.84E–06	9.43E–06
Thyroid	1.93E–22	2.89E–22	3.85E–22	2.07E–12	4.94E–09	9.01E–08
Total body	1.37E–04	2.04E–04	1.17E–04	1.02E–04	6.75E–05	5.80E–05

Source	Photon energy (MeV)					
	0.200	0.500	1.000	1.500	2.000	4.000
Bladder	2.25E–04	1.79E–04	1.12E–04	1.91E–04	1.37E–04	1.22E–04
Stomach	1.27E–05	1.41E–05	4.21E–05	2.50E–05	2.37E–05	2.00E–05
Small intestine	3.10E–04	2.48E–04	2.80E–04	1.91E–04	1.76E–04	2.32E–04
Upper large intestine	3.39E–04	3.63E–04	1.91E–04	1.55E–04	2.75E–04	1.72E–04
Lower large intestine	5.90E–04	4.48E–04	4.55E–04	4.15E–04	3.83E–04	2.90E–04
Kidneys	3.67E–05	3.27E–05	4.49E–05	3.17E–05	2.97E–05	1.46E–07
Liver	1.49E–05	5.40E–06	2.06E–05	2.84E–05	1.84E–05	1.59E–05
Lungs	3.65E–06	4.37E–06	4.75E–06	4.85E–06	4.91E–06	4.61E–06
Other tissue (muscle)	5.81E–05	5.66E–05	5.29E–05	4.96E–05	4.67E–05	3.93E–05
Ovaries	2.05E–02	2.17E–02	2.00E–02	1.89E–02	1.75E–02	1.42E–02
Pancreas	9.43E–06	1.06E–05	2.89E–05	1.96E–05	1.86E–05	1.60E–05
Skeleton	2.03E–05	3.10E–05	2.61E–05	2.31E–05	2.27E–05	1.84E–05
Skin	1.46E–05	8.44E–06	1.74E–05	1.45E–05	1.74E–05	1.01E–05
Spleen	1.70E–05	3.06E–05	1.41E–05	1.79E–05	2.86E–06	8.20E–07
Thyroid	2.48E–07	5.14E–07	7.96E–07	9.68E–07	1.08E–06	1.25E–06
Total body	5.38E–05	4.83E–05	3.47E–05	5.43E–05	5.08E–05	5.35E–05

[a]Read as 5.15×10^{-8}.

Source: ICRP 1975.

Table G–4 (cont'd) Fraction of photon energy released in source organ and absorbed in small intestine, based on ICRP Publication 23.

Target: Small Intestine

Source	Photon energy (MeV)					
	0.010	0.015	0.020	0.030	0.050	0.100
Bladder	1.58E–07[a]	2.37E–07	1.83E–04	5.31E–03	1.29E–02	1.27E–02
Stomach	2.07E–04	3.11E–04	1.28E–03	6.99E–03	1.27E–02	1.12E–02
Small intestine	7.70E–01	6.87E–01	5.82E–01	3.86E–01	1.94E–01	1.18E–01
Upper large intestine	5.68E–03	5.26E–02	1.24E–01	1.56E–01	1.07E–01	6.75E–02
Lower large intestine	2.52E–03	2.89E–02	6.39E–02	8.12E–02	5.64E–02	3.80E–02
Kidneys	6.77E–06	1.02E–05	1.00E–03	6.74E–03	1.28E–02	1.19E–02
Liver	1.68E–04	2.53E–04	8.01E–04	3.07E–03	6.65E–03	6.57E–03
Lungs	1.72E–14	2.57E–14	3.04E–08	4.86E–05	3.74E–04	7.39E–04
Other tissue (muscle)	7.24E–04	2.23E–03	4.41E–03	7.60E–03	7.79E–03	6.19E–03
Ovaries	2.98E–03	2.32E–02	6.15E–02	9.83E–02	7.51E–02	4.99E–02
Pancreas	2.69E–08	4.05E–08	4.17E–05	1.94E–03	6.65E–03	7.39E–03
Skeleton	1.58E–04	2.37E–04	5.21E–04	1.76E–03	3.21E–03	2.92E–03
Skin	6.71E–05	1.01E–04	1.34E–04	8.99E–04	1.79E–03	1.76E–03
Spleen	1.84E–07	2.76E–07	9.77E–05	1.55E–03	5.28E–03	5.82E–03
Testes	2.78E–15	4.17E–15	1.68E–08	4.85E–05	8.36E–04	1.30E–03
Thyroid	4.76E–32	7.14E–32	1.12E–16	5.47E–09	3.63E–06	2.05E–05
Total body	1.50E–02	1.51E–02	1.45E–02	1.39E–02	1.03E–02	7.86E–03

Source	Photon energy (MeV)					
	0.200	0.500	1.000	1.500	2.000	4.000
Bladder	1.07E–02	9.33E–03	9.19E–03	8.50E–03	8.76E–03	6.92E–03
Stomach	9.64E–03	9.44E–03	8.49E–03	7.66E–03	7.97E–03	6.64E–03
Small intestine	1.11E–01	1.11E–01	9.95E–02	9.43E–02	8.56E–02	6.95E–02
Upper large intestine	6.13E–02	5.83E–02	5.25E–02	4.72E–02	4.38E–02	3.42E–02
Lower large intestine	3.45E–02	3.19E–02	2.95E–02	2.75E–02	2.61E–02	2.07E–02
Kidneys	1.06E–02	9.80E–03	9.38E–03	9.27E–03	8.37E–03	6.93E–03
Liver	6.25E–03	5.66E–03	5.37E–03	5.30E–03	4.83E–03	4.33E–03
Lungs	7.43E–04	9.95E–04	1.12E–03	1.08E–03	1.21E–03	1.15E–03
Other tissue (muscle)	5.73E–03	5.54E–03	5.20E–03	4.92E–03	4.61E–03	3.92E–03
Ovaries	4.36E–02	4.23E–02	3.71E–02	3.47E–02	3.28E–02	2.61E–02
Pancreas	6.94E–03	6.30E–03	6.14E–03	5.84E–03	5.48E–03	4.70E–03
Skeleton	2.84E–03	2.88E–03	2.90E–03	2.45E–03	2.44E–03	2.06E–03
Skin	1.80E–03	1.98E–03	2.09E–03	2.01E–03	1.87E–03	1.62E–03
Spleen	5.28E–03	4.96E–03	4.75E–03	4.86E–03	4.26E–03	3.69E–03
Testes	1.56E–03	1.92E–03	1.85E–03	1.85E–03	1.93E–03	1.64E–03
Thyroid	6.03E–05	2.57E–05	1.44E–04	1.99E–04	2.00E–04	2.12E–04
Total body	7.29E–03	7.08E–03	6.56E–03	6.08E–03	5.62E–03	5.01E–03

[a]Read as 1.58×10^{-7}.

Source: ICRP 1975.

Table G–4 (cont'd) Fraction of photon energy released in source organ and absorbed in upper large intestine, based on ICRP Publication 23.

Target: Upper Large Intestine

Source	Photon energy (MeV)					
	0.010	0.015	0.020	0.030	0.050	0.100
Bladder	3.57E–08[a]	5.37E–08	2.13E–05	6.35E–04	1.80E–03	1.74E–03
Stomach	1.69E–04	2.53E–04	1.19E–03	3.39E–03	3.97E–03	2.93E–03
Small intestine	9.41E–02	9.36E–02	8.26E–02	5.73E–02	2.97E–02	1.81E–02
Upper large intestine	7.59E–02	1.67E–01	1.80E–01	1.16E–01	5.45E–02	3.18E–02
Lower large intestine	2.15E–03	4.64E–03	6.60E–03	6.42E–03	4.62E–03	3.36E–03
Kidneys	1.56E–07	2.34E–07	7.73E–05	1.31E–03	2.45E–03	2.36E–03
Liver	3.95E–05	5.94E–05	3.57E–04	1.79E–03	2.47E–03	2.11E–03
Lungs	5.29E–15	7.94E–15	9.45E–09	1.61E–05	1.07E–04	1.75E–04
Other tissue (muscle)	9.15E–04	1.01E–03	1.30E–03	1.72E–03	1.62E–03	1.28E–03
Ovaries	1.87E–03	1.41E–02	2.26E–02	2.15E–02	1.33E–02	8.69E–03
Pancreas	8.11E–09	1.22E–08	1.27E–05	5.83E–04	1.73E–03	1.74E–03
Skeleton	4.43E–05	6.63E–05	1.35E–04	2.88E–04	5.37E–04	5.35E–04
Skin	2.63E–05	3.95E–05	5.27E–05	2.49E–04	4.08E–04	3.82E–04
Spleen	2.47E–08	3.70E–08	1.40E–05	4.56E–04	1.24E–03	1.30E–03
Testes	2.82E–15	4.24E–15	5.75E–09	9.99E–06	1.40E–04	2.22E–04
Thyroid	1.95E–32	2.93E–32	3.93E–17	1.48E–09	8.78E–07	9.09E–06
Total body	3.07E–03	3.16E–03	2.80E–03	2.84E–03	2.03E–03	1.54E–03

Source	Photon energy (MeV)					
	0.200	0.500	1.000	1.500	2.000	4.000
Bladder	1.75E–03	1.71E–03	1.29E–03	1.29E–03	1.21E–03	1.11E–03
Stomach	2.63E–03	2.36E–03	2.01E–03	2.45E–03	1.76E–03	1.65E–03
Small intestine	1.72E–02	1.64E–02	1.51E–02	1.40E–02	1.32E–02	1.04E–02
Upper large intestine	3.07E–02	3.07E–02	2.91E–02	2.59E–02	2.47E–02	1.95E–02
Lower large intestine	3.14E–03	3.03E–03	2.61E–03	2.82E–03	2.26E–03	2.06E–03
Kidneys	2.15E–03	2.07E–03	1.92E–03	1.93E–03	1.52E–03	1.31E–03
Liver	1.82E–03	1.85E–03	1.61E–03	1.36E–03	1.45E–03	1.09E–03
Lungs	1.79E–04	2.76E–04	2.88E–04	3.03E–04	2.86E–04	3.66E–04
Other tissue (muscle)	1.20E–03	1.17E–03	1.11E–03	1.05E–03	9.78E–04	8.30E–04
Ovaries	8.34E–03	7.98E–03	7.02E–03	6.67E–03	6.21E–03	4.62E–03
Pancreas	1.66E–03	1.55E–03	1.50E–03	1.41E–03	1.24E–03	1.05E–03
Skeleton	5.58E–04	5.02E–04	5.45E–04	4.87E–04	4.85E–04	3.70E–04
Skin	3.47E–04	4.18E–04	4.70E–04	3.72E–04	3.89E–04	3.01E–04
Spleen	9.11E–04	1.01E–03	9.57E–04	9.68E–04	9.72E–04	6.33E–04
Testes	2.78E–04	2.30E–04	2.93E–04	2.42E–04	4.81E–04	2.97E–04
Thyroid	8.42E–06	7.59E–06	3.16E–05	4.79E–05	3.87E–05	8.19E–05
Total body	1.32E–03	1.41E–03	1.26E–03	1.12E–03	1.08E–03	8.84E–04

[a]Read as 3.57×10^{-8}.

Source: ICRP 1975.

Table G–4 (cont'd) Fraction of photon energy released in source organ and absorbed in lower large intestine, based on ICRP Publication 23.

Target: Lower Large Intestine

Source	Photon energy (MeV)					
	0.010	0.015	0.020	0.030	0.050	0.100
Bladder	5.47E–05[a]	8.19E–05	1.25E–03	5.62E–03	6.66E–03	4.82E–03
Stomach	2.74E–07	4.10E–07	4.48E–05	2.93E–04	7.65E–04	7.10E–04
Small intestine	4.50E–03	8.19E–03	1.09E–02	1.01E–02	6.85E–03	4.51E–03
Upper large intestine	3.95E–04	5.92E–04	1.82E–03	2.90E–03	2.42E–03	2.08E–03
Lower large intestine	8.85E–02	1.81E–01	1.86E–01	1.12E–01	4.75E–02	2.82E–02
Kidneys	1.33E–09	1.98E–09	1.86E–06	1.06E–04	2.90E–04	3.98E–04
Liver	4.37E–15	6.56E–15	3.23E–09	4.24E–06	5.34E–05	1.40E–04
Lungs	1.00E–17	1.50E–17	1.81E–10	1.17E–06	1.33E–05	2.85E–05
Other tissue (muscle)	1.09E–05	2.16E–04	6.59E–04	1.27E–03	1.32E–03	1.04E–03
Ovaries	1.59E–03	1.30E–02	2.34E–02	2.32E–02	1.42E–02	8.99E–03
Pancreas	2.26E–12	3.39E–12	1.41E–07	4.93E–05	2.77E–04	3.55E–04
Skeleton	1.04E–04	1.55E–04	2.94E–04	5.54E–04	6.56E–04	6.35E–04
Skin	9.15E–06	1.37E–05	1.82E–05	1.45E–04	2.64E–04	2.94E–04
Spleen	2.91E–10	4.37E–10	9.25E–07	7.28E–05	3.22E–04	3.76E–04
Testes	2.08E–07	3.12E–07	1.26E–04	1.10E–03	2.10E–03	1.70E–03
Thyroid	1.33E–35	2.00E–35	4.40E–19	9.06E–11	1.06E–07	1.60E–06
Total body	2.34E–03	1.94E–03	2.19E–03	2.02E–03	1.66E–03	1.07E–03

Source	Photon energy (MeV)					
	0.200	0.500	1.000	1.500	2.000	4.000
Bladder	4.02E–03	3.90E–03	3.34E–03	3.46E–03	3.23E–03	2.18E–03
Stomach	7.44E–04	6.96E–04	7.25E–04	7.22E–04	6.37E–04	4.42E–04
Small intestine	4.03E–03	3.71E–03	3.50E–03	3.25E–03	3.28E–03	2.61E–03
Upper large intestine	1.70E–03	1.65E–03	1.73E–03	1.38E–03	1.30E–03	9.58E–04
Lower large intestine	2.78E–02	2.83E–02	2.59E–02	2.43E–02	2.22E–02	1.73E–02
Kidneys	4.88E–04	4.85E–04	4.54E–04	5.42E–04	4.69E–04	4.03E–04
Liver	1.37E–04	1.79E–04	1.42E–04	1.98E–04	1.52E–04	2.24E–04
Lungs	6.48E–05	4.30E–05	5.14E–05	3.41E–05	3.74E–05	4.30E–05
Other tissue (muscle)	9.62E–04	9.34E–04	8.77E–04	8.29E–04	7.82E–04	6.54E–04
Ovaries	8.11E–03	7.81E–03	6.80E–03	6.43E–03	6.14E–03	5.39E–03
Pancreas	3.30E–04	2.94E–04	2.96E–04	3.73E–04	2.46E–04	3.06E–04
Skeleton	6.11E–04	5.18E–04	5.73E–04	4.85E–04	4.35E–04	4.06E–04
Skin	2.85E–04	3.33E–04	3.60E–04	3.06E–04	3.33E–04	2.32E–04
Spleen	3.63E–04	3.86E–04	3.30E–04	3.38E–04	3.55E–04	2.90E–04
Testes	1.59E–03	1.57E–03	1.16E–03	1.28E–03	1.17E–03	1.18E–03
Thyroid	4.14E–06	8.35E–06	1.29E–05	1.59E–05	1.78E–05	2.08E–05
Total body	9.47E–04	1.09E–03	1.02E–03	9.42E–04	1.14E–03	6.45E–04

[a]Read as 5.47×10^{-5}.

Source: ICRP 1975.

3. You are the director of a radiochemistry laboratory and a client has requested the analysis of Sr-89 in vegetation with a Minimum Detectable Concentration (MDC) of 1.0 pCi/g of dry sample. The laboratory is equipped with a full array of analytical instruments including a gas-flow proportional counter for Sr-89 measurements.

   Outline a radiochemical method of analysis indicating your choice of sample pretreatment, concentration, purification/separation, and discuss three measures to ensure the quality of the individual results.

   Determine whether the MDC is met based on the following assumptions: a detector counting efficiency for Sr-89 of 45%, an average background of 1 cpm, a counting time of 50 minutes, and a chemical yield of 75%. Round your calculation (s) to two significant figures.

   Disregard the presence of other strontium isotopes, and radioactive decay between sampling and counting.

4. A worker is believed to have received a significant amount of radiation exposure during the recent criticality accident at the nuclear fuel conversion facility in Tokai, Japan. You are to assess the effective dose equivalent (H_E) of the worker due to the accident. The following information is given:

   a. During the accident, the worker has worked 3 minutes at a distance of 20 meters from the fuel-mixing tank that went critical.
   b. The worker did not wear a personnel dosimeter.
   c. The amount of ^{24}Na in the worker's blood is too low to tell the neutron exposure.
   d. There is a negligible amount of radiation shield between the fuel-mixing tank and the site boundary (50 meters away).
   e. The average reading of gamma-ray monitor at the site boundary during the accident is 2 mSv hr^{-1}.
   f. The radiation dose is mainly contributed from the prompt $^{235}(n_{th},fission)$ reactions, and the spectra of the gamma rays and neutrons emitted from the prompt fission reactions are given in the Attachment.
   g. The conversion factors of neutron fluence-to-dose equivalent are also provided in the Attachment.

(see 5 pages of attachments.)

an energy increment are discussed in Sec. 2.2.2. In particular, the average energy is often used, in which case the integral of Eq. 2.2-16 is carried out over the range of the energy increment.

For many purposes an average energy will not suffice, and the actual energy distribution must be carried through the analysis from source to detector. The term *spectrum* is used interchangeably with energy distribution, following the practice of the spectroscopist.

2.4.1 Energy Distributions of Gamma-Ray Sources

A few relevant characteristics of the spectra of gamma-ray sources encountered in reactors were included in the discussion of the various source types (Sec. 2.1.1). The two most important sources are the prompt fission reactions and fission products; their energy spectra are discussed in the following two sections. Capture and inelastic neutron-scattering gamma-ray spectral data are given in Appendix A.

(a) **Prompt Fission Gamma-Ray Spectra.** The spectrum of gamma rays given off simultaneously with the fission of ^{235}U has been rather extensively studied. The measurements of Peelle and Maienschein[2] are the most accurate published data; they contain uncertainties of at most 15%, and, in most energy regions, the uncertainty is less. Figure 2.15 presents the differential energy distribution (photons fission^{-1} MeV^{-1}) measured by Peelle and Maienschein.[6] Kirkbride[7] found that the spectra for ^{233}U and ^{234}Pu were not significantly different from that for ^{235}U. Even ^{252}Cf, which fissions spontaneously, exhibits a prompt gamma-ray spectrum very similar to that of ^{235}U (Ref. 8). The spectrum of Fig. 2.15 may be approximated by the segmented fit:

$$\Gamma(E) = \begin{cases} 6.6 & 0.1 < E < 0.6 \text{ MeV} \\ 20.2 \exp(-1.78E) & 0.6 < E < 1.5 \text{ MeV} \\ 7.2 \exp(-1.09E) & 1.5 < E < 10.5 \text{ MeV} \end{cases} \qquad (2.4\text{-}1)$$

The equation agrees with the experimental spectrum plus uncertainty to within 10% from 0.6 to 7.5 MeV except at 1.2 and ~5.0 MeV, where it deviates ~16%. The constant yield agrees with experiment from 0.1 to 0.6 MeV to within ~20% except at 0.26 MeV. An approximation for the energy region from 0.01 to 0.6 MeV, which may be adequate for shielding

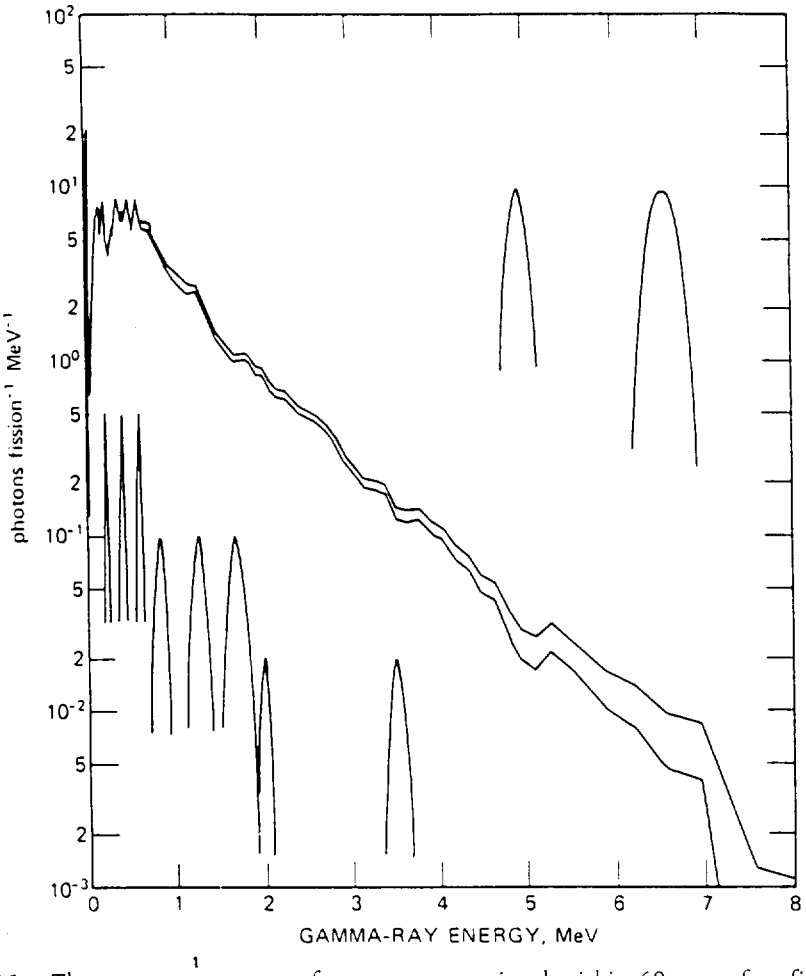

Fig. 2.15—The energy spectrum of gamma rays emitted within 69 nsec after fission of ^{235}U by thermal neutrons. The two lines, which represent the random (largely propagated from counting statistics) 2/3 confidence limits on the spectrum, are drawn as straight lines between adjacent mean window energies. The nearly Gaussian shapes shown at the lower left and upper right indicate the energy resolution (From Peelle and Maienschein.[6])

calculations, is the emission of 3.75 photons/fission of average energy 0.324 MeV.

Although the approximation of Eq. 2.4-1 is useful, for most applications accuracy demands the use of a numerical representation of the spectrum rather than these less-precise analytical functions. Photon yields per fission in fine and broad energy groups are given in Appendix A.

ingly better with measurements as the number of identified decay chains increases. Perhaps the most authoritative work was published by Perkins and King[11] and later updated by Perkins.[12] The results of the later work are given in Appendix A. For instantaneous fission and 1, 10, 100, and 1000 hr of reactor operation, these data give disintegration rate, beta-ray energy release, and total gamma-ray energy release and further subdivide the gamma rays into seven energy intervals. Unfortunately, the uppermost energy interval contains everything above 2.6 MeV. Results calculated by Scoles[13] avoid this shortcoming since his energy intervals are 1 MeV wide, except the topmost, which contains only one line at 5.4 MeV. These results were used considerably for some years since they were uniquely suited to shielding problems for times to 10^6 hr of reactor operation and to 10^4 hr after shutdown. Perhaps a reader of this text will update this work.

For approximate calculations the total fission-product decay rate is given within 20% from 10 min to 30 days after fission by Goldstein[14]

$$\Gamma_T(t) = 1.5t^{-1.2} \text{ MeV fission}^{-1} \text{ sec}^{-1} \qquad (2.4\text{-}3)$$

where t is the time (in seconds) after fission.

2.4.2 Neutron Spectra from Fission

The energy distribution of neutrons from fission is obviously one of the principal inputs in the preparation of the source term for a reactor. The energy range of importance in shielding for thermal fission in ^{235}U, 3 to 17 MeV, was measured by Watt,[15] who also reviewed measurements by others in lower ranges and proposed an empirical expression to fit the data from 0.075 to 17 MeV:

$$N(E) = 0.484e^{-E} \sinh (2E)^{\frac{1}{2}} \text{ neutrons MeV}^{-1} \text{ fission}^{-1} \qquad (2.4\text{-}4)$$

where $N(E)$ is the fraction of neutrons per unit energy interval emitted per fission and E is neutron energy in MeV. The Watt fission spectrum was widely used until Cranberg, Frye, Nereson, and Rosen[16] reported new measurements from 0.18 to 12 MeV.

These results were based on time-of-flight measurements to about 8 MeV and photographic emulsion exposures to 12 MeV. Cranberg et al. reported that

$$N(E) = 0.453e^{-E/0.965} \sinh (2.29E)^{\frac{1}{2}} \text{ neutrons MeV}^{-1} \text{ fission}^{-1} \quad (2.4\text{-}5)$$

was a more accurate fit over the entire range.

Note, however, that uncertainties in the measurements, 15% or less to 8 MeV, were 30% or more at 12 MeV and above. Equation 2.4-5 is plotted in Fig. 2.18 and tabulated for numerical use in Ref. 14. The tabulation

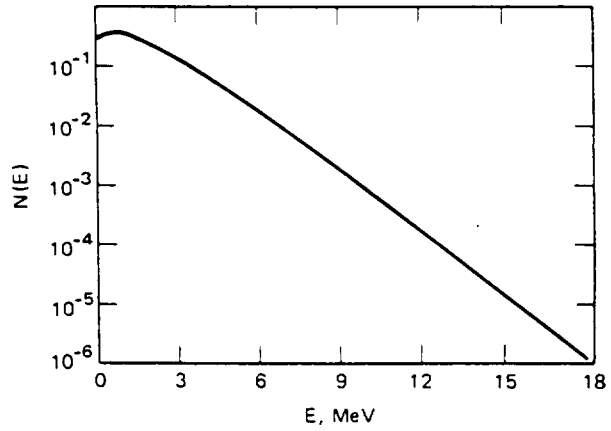

Fig. 2.18—Fraction of neutrons per MeV interval emitted at energy E from the thermal fission of ^{235}U. (From Herbert Goldstein, *Reactor Handbook*, Second Edition, Vol. III, Part B, Shielding, E. P. Blizard (Ed.), p. 19, Interscience Publishers, a division of John Wiley & Sons, Inc., New York, 1962.)

also gives the fraction of neutrons above E and the energy per fission carried by neutrons above E.

An even simpler expression that is within 15% of Eq. 2.4-5 over its range of validity (and within 7%, $5 < E < 13$ MeV) is due to Goldstein:[14]

$$N(E) = 1.75e^{-0.766E} \text{ neutrons MeV}^{-1} \text{ fission}^{-1}$$

$$(4 < E < 14 \text{ MeV}) \quad (2.4\text{-}6)$$

This form is very convenient in analytical manipulations and adequately covers the energy range of greatest interest in many reactor shielding problems.

Both the spectrum and the total number of neutrons evolved in fission vary with the energy of the incident neutron and with the species of fissionable material. In experiments at Los Alamos, Grundl and Neuer[17] and

Table 17. Effective dose equivalent per unit fluence for neutrons incident in various geometries on an anthropomorphic phantom

Neutron energy, MeV	Conversion coefficient, 10^{-12} Sv cm^2			
	AP	PA	LAT	ROT
$2.5\ 10^{-8}$	(4.00)	(2.60)	(1.30)	(2.30)
$1.0\ 10^{-7}$	(4.40)	(2.70)	(1.40)	(2.40)
$1.0\ 10^{-6}$	4.82	2.81	1.43	2.63
$1.0\ 10^{-5}$	4.46	2.78	1.33	2.48
$1.0\ 10^{-4}$	4.14	2.63	1.27	2.33
$1.0\ 10^{-3}$	3.83	2.49	1.19	2.18
$1.0\ 10^{-2}$	4.53	2.58	1.27	2.41
$2.0\ 10^{-2}$	5.87	2.79	1.46	2.89
$5.0\ 10^{-2}$	10.9	3.64	2.14	4.70
$1.0\ 10^{-1}$	19.8	5.69	3.57	8.15
$2.0\ 10^{-1}$	38.6	8.60	6.94	15.3
$5.0\ 10^{-1}$	87.0	30.8	18.7	38.8
$1.0\ 10^{0}$	143	53.5	33.3	65.7
$1.5\ 10^{0}$	183	85.8	52.1	93.7
$2.0\ 10^{0}$	214	120	71.8	120
$3.0\ 10^{0}$	264	174	105	162
$4.0\ 10^{0}$	300	215	131	195
$5.0\ 10^{0}$	327	244	151	219
$6.0\ 10^{0}$	347	265	167	237
$7.0\ 10^{0}$	365	283	181	253
$8.0\ 10^{0}$	380	296	194	266
$1.0\ 10^{1}$	410	321	218	292
$1.4\ 10^{1}$	(480)	(415)	(280)	(365)

See Section 3.6 for irradiation geometries.

These values of the conversion coefficient relate to the dose equivalent for neutrons as defined before 1985. They should be multiplied by a factor of 2 to obtain the dose equivalent as redefined for neutrons in 1985 (ICRP, 1985).

Values in parentheses are extrapolated from original data.

5. An individual accidentally ingested a certain amount of ^{137}Cs. A whole-body counting measured 1.0×10^5 Bq of ^{137}Cs immediately after the event. Assume class D for the ingested cesium, use the attached decay and metabolic data and the gamma-ray absorption fractions to estimate $H_{E,50}$.

(See 13 attached pages for problems 5 and 6)

^{137}Cs 30.0 y

Radioactive Daughter		Half Life
^{137m}Ba	(94.6%)	2.552 min

Principal Beta Particles

Frequency (%)	Avg E (keV)	Max E (keV)
94.43	173.4	511.5
5.57	424.6	1173.2
keV/decay	187.4	

^{137m}Ba 2.552 min

Principal Conversion and Auger Electrons

Frequency (%)	Energy (keV)
8.32	624.2
1.19	655.7
keV/decay	65.1 *

Principal Gamma and X Rays

Frequency (%)	Energy (keV)
2.13	31.8
3.92	32.2
89.78	661.6
keV/decay	596.5

5. DOSIMETRIC MODEL FOR THE RESPIRATORY SYSTEM

5.1. Introduction

The dosimetric model developed in this Chapter relates to the inhalation of radioactive aerosols. The special cases of gas and free ion deposition will receive further consideration. Some special cases will be referred to in the metabolic data for individual elements and also Chapter 8.

When radioactive aerosols are inhaled, parts of the respiratory system are irradiated. Other organs and tissues of the body are also irradiated both by radiations originating from the lungs and as a result of translocation of inhaled material to body tissues from the respiratory system.

It is recognized that after the inhalation of radioactive aerosols the doses received by various regions of the respiratory system will differ widely, depending on the size distribution of the inhaled material. In this report the dose received by the nasopharyngeal region has been neglected since for most particle sizes it is usually small in comparison with the doses received by other regions. The dose delivered to some of the pulmonary lymph nodes by insoluble particles cleared from the pulmonary region may be many times greater than that received by the lung tissues. However, from considerations of the possible effects in the whole lymphoid tissue, of which the pulmonary lymph nodes form only a part, and of autopsy data on men who had inhaled particles of plutonium, the Commission has decided that irradiation of the lung is likely to be more limiting than that of lymphoid tissue for inhaled, insoluble, radioactive particles (paras. 52 and 53, *ICRP Publication 26*). The distribution of dose to cells in the lung from inhaled particles may also be very inhomogeneous. For the induction of malignant disease, the Commission considers that the hazard of radioactive particles in the lung is likely to be less than that of the same amount of material distributed uniformly in the lung (paras. 49 and 50, *ICRP Publication 26*). Although in principle the model described here could be used to estimate dose equivalent in the different regions of the respiratory system, and this might be useful for research, In view of other uncertainties, e.g. concerning the precise location of the cells at risk, it is not considered that such estimates are yet warranted for fixing values of ALI. Therefore, for the purposes of radiological protection, the Commission considers that in adults it will be satisfactory to consider the tracheobronchial region, pulmonary region and pulmonary lymph nodes as one composite organ of mass 1 000 g (para. 54, *ICRP Publication 26*) to which the weighting factor for lung given in Table 2.1 applies.

As explained in previous chapters, the exposure of workers to radioactive materials is limited by consideration of the committed dose equivalents H_{50} in the tissues of the body. The method used to calculate H_{50} has been described in Chapter 4 where it is explained that H_{50} for any target organ depends on U_S, the total number of transformations in a source organ over the 50 years following intake of the radionuclide, and SEE($T \leftarrow S$), the specific effective energy absorbed in a target organ from each type of radiation arising in a source organ. The methods used to calculate U_S and SEE($T \leftarrow S$) for parts of the respiratory system, and to calculate H_{50} for the composite lung tissue defined above, are described below.

5.2. Deposition and Retention Model

Estimates of the distribution and retention of material in the respiratory system are based on a model proposed in the report of the ICRP Task Group on Lung Dynamics (1966). This

model takes account of particle size and also defines three classes of retention which, in part, reflect the chemical form of the aerosol. Additionally the model provides information on the various routes of elimination from the lungs. Although further consideration by the Task Group and Committee 2 since publication of the report on lung dynamics has resulted in many changes in values of the deposition and clearance parameters, the model is substantially that of the Task Group (see also *ICRP Publication* 19).

The respiratory system is divided into three distinct regions—the nasal passage (N–P), the trachea and bronchial tree (T–B) and the pulmonary parenchyma (P). Deposition is assumed to vary with the aerodynamic properties of the aerosol distribution and is described by the three parameters D_{N-P}, D_{T-B}, and D_P which represent the fractions of inhaled material initially deposited in the N–P, T–B, and P regions, respectively. For a log-normal distribution of diameters, which seems typical of aerosols, the pattern of deposition can be related to the activity median aerodynamic diameter (AMAD) of the aerosol (Fig. 5.1). In this report calculations of committed dose equivalent are for an aerosol with an AMAD of 1 μm. Estimates for other AMADs can be made using the data in Fig. 5.1 as discussed in Section 5.5 below.

To describe the clearance of inhaled radioactive materials from the lung, materials are classified as D, W or Y which refer to their retention in the pulmonary region. This classification applies to a range of half-times for D of less than 10 days, for W from 10 to 100 days and for Y greater than 100 days. The three regions, N–P, T–B and P described above are each divided into two or four compartments as shown in Fig. 5.2. Each of these compartments is

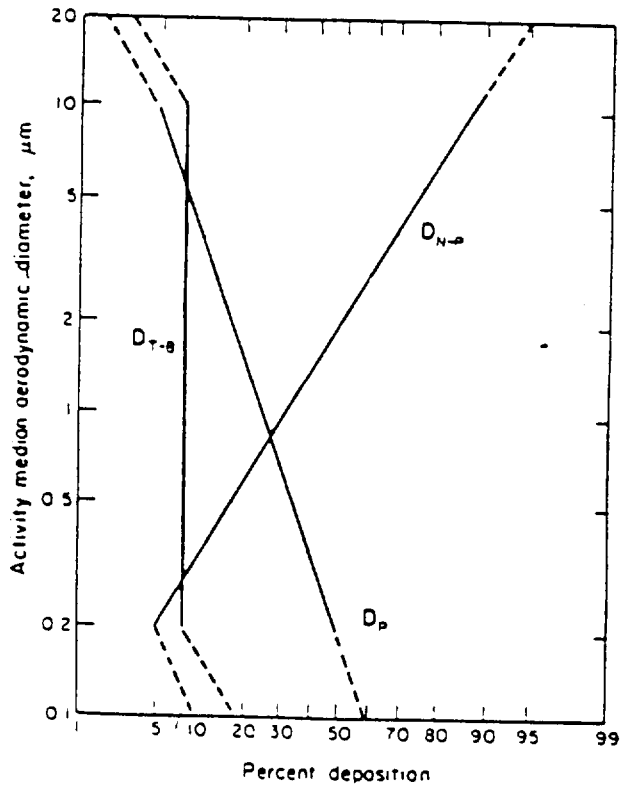

Fig. 5.1. Deposition of dust in the respiratory system. The percentage of activity or mass of an aerosol which is deposited in the N–P, T–B and P regions is given in relation to the Activity Median Aerodynamic Diameter (AMAD) of the aerosol distribution. The model is intended for use with aerosol distributions with AMADs between 0.2 and 10 μm and with geometric standard deviations of less than 4.5. Provisional estimates of deposition further extending the size range are given by the dashed lines. For an unusual distribution with an AMAD of greater than 20 μm, complete deposition in N–P can be assumed. The model does not apply to aerosols with AMADs of less than 0.1 μm.

Region	Compartment	Class D T day	D F	Class W T day	W F	Class Y T day	Y F
N–P (D_{N-P} = 0.30)	a	0.01	0.5	0.01	0.1	0.01	0.01
	b	0.01	0.5	0.40	0.9	0.40	0.99
T–B (D_{T-B} = 0.08)	c	0.01	0.95	0.01	0.5	0.01	0.01
	d	0.2	0.05	0.2	0.5	0.2	0.99
P (D_P = 0.25)	e	0.5	0.8	50	0.15	500	0.05
	f	n.a.	n.a.	1.0	0.4	1.0	0.4
	g	n.a.	n.a.	50	0.4	500	0.4
	h	0.5	0.2	50	0.05	500	0.15
L	i	0.5	1.0	50	1.0	1 000	0.9
	j	n.a.	n.a.	n.a.	n.a.	∞	0.1

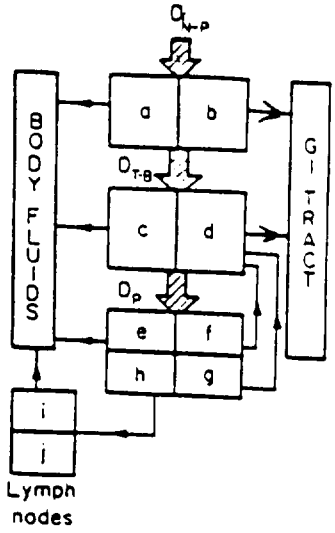

Fig. 5.2. Mathematical model used to describe clearance from the respiratory system. The values for the removal half-times, T_{s-i} and compartmental fractions, F_{s-i} are given in the tabular portion of the figure for each of the three classes of retained materials. The values given for D_{N-P}, D_{T-B} and D_P (left column) are the regional depositions for an aerosol with an AMAD of 1 μm. The schematic drawing identifies the various clearance pathways from compartments a–i in the four respiratory regions, N–P, T–B, P and L.
n.a. = not applicable.

associated with a particular pathway of clearance for which the half-time of clearance is T days and the fraction leaving the region by that rate is F. Thus, compartments a, c and e are associated with absorption processes, whereas b, d, f and g are associated with particle transport processes, including mucociliary transport, which translocate material to the gastrointestinal tract. The pulmonary lymphatic system (L) also serves to remove dust from the lungs. It is associated with compartment h in the P region of the lungs from which material is translocated to compartments i and j in the pulmonary lymph nodes. Material in compartment i is translocated to body fluids but that in compartment j is assumed to be retained there indefinitely. This compartment is only considered appropriate for class Y aerosols; for class D and W aerosols the fraction of material entering compartment j from compartment h (F_j) is set equal to zero. The clearance of material from each of the compartments described above is assumed to be governed by first order kinetics so that each compartment is associated with a clearance constant λ and half-time of clearance $T = 0.693/86\,400\,\lambda$. The clearance of inhaled material from the lung is, therefore, described by a set of interlinked first order differential equations, as follows

$$\frac{d}{dt} q_a(t) = I(t) \cdot D_{N-P} \cdot F_a - \lambda_a q_a(t) - \lambda_R q_a(t) \tag{5.1a}$$

$$\frac{d}{dt} q_b(t) = I(t) \cdot D_{N-P} \cdot F_b - \lambda_b q_b(t) - \lambda_R q_b(t) \tag{5.1b}$$

$$\frac{d}{dt} q_c(t) = I(t) \cdot D_{T-B} \cdot F_c - \lambda_c q_c(t) - \lambda_R q_c(t) \tag{5.1c}$$

$$\frac{d}{dt} q_d(t) = I(t) \cdot D_{T-B} \cdot F_d + \lambda_f q_f(t) + \lambda_g q_g(t) - \lambda_d q_d(t) - \lambda_R q_d(t) \tag{5.1d}$$

$$\frac{d}{dt} q_e(t) = I(t) \cdot D_P \cdot F_e - \lambda_e q_e(t) - \lambda_R q_e(t) \quad (5.1e)$$

$$\frac{d}{dt} q_f(t) = I(t) \cdot D_P \cdot F_f - \lambda_f q_f(t) - \lambda_R q_f(t) \quad (5.1f)$$

$$\frac{d}{dt} q_g(t) = I(t) \cdot D_P \cdot F_g - \lambda_g q_g(t) - \lambda_R q_g(t) \quad (5.1g)$$

$$\frac{d}{dt} q_h(t) = I(t) \cdot D_P \cdot F_h - \lambda_h q_h(t) - \lambda_R q_h(t) \quad (5.1h)$$

$$\frac{d}{dt} q_i(t) = F_i \lambda_h q_h(t) - \lambda_i q_i(t) - \lambda_R q_i(t) \quad (5.1i)$$

$$\frac{d}{dt} q_j(t) = F_j \lambda_h q_h(t) - \lambda_R q_j(t) \quad (5.1j)$$

where $q_a(t)$, $q_b(t)$, etc. are the activities of an inhaled radionuclide in compartment a, b, etc. at time t;

$I(t)$ is the rate of inhalation of activity of the radionuclide;

λ_a to λ_i are the biological clearance rates of compartments a to i;

λ_R is the radioactive decay constant of the radionuclide, and

F_a to F_j are the fractions of material entering the various regions of the lung that are associated with the various compartments contained therein.

Values of F_a to F_j are given in Fig. 5.2 for the various inhalation classes D, W and Y. Also given are T_a to T_i for these various classes. λ_a to λ_i are obtained from the values of T_a to T_i by use of the formula $\lambda = 0.693/86\,400T$,

where λ is in s^{-1};

T is in days, and

86 400 is the number of seconds in a day.

The classification D, W or Y for different chemical forms of a radionuclide are given in the metabolic data for the individual elements. As stated in Chapter 4 it is assumed that radioactive daughters remain with and behave metabolically like the inhaled parent radionuclide. In fact, there is a paucity of evidence about the behaviour of radioactive daughters produced within the lung. However, it is at least plausible to assume that daughters produced within a radioactive particle stay within the particle. The build-up and clearance of a radioactive daughter produced in the different compartments of the lung is, therefore, governed by a series of first order differential equations similar to those given in eqn (5.1). If $q'(t)$ is the activity of the radioactive daughter in any compartment at time t and $q(t)$ is the activity of its immediate precursor, then

$$\frac{d}{dt} q'_a(t) = \lambda'_R q_a(t) - \lambda_a q'_a(t) - \lambda'_R q'_a(t) \quad (5.2a)$$

6. DOSIMETRIC MODEL FOR THE GASTROINTESTINAL TRACT

6.1. Introduction

As explained in previous chapters of this report, exposure of workers to a radioactive material is limited by consideration of the committed dose equivalent H_{50} received by organs and tissues of the body following intake of the radionuclide concerned. The general method used to calculate H_{50} has been discussed in Chapter 4, where it was explained that $H_{50,T}$ in a target organ T depends on U_S, the number of transformations in source organ S over the 50 years following intake of the radionuclide and SEE($T \leftarrow S$), the specific effective energy absorbed in target organ T from radiations originating in source organ S. The methods used to calculate U_S, SEE($T \leftarrow S$) and $H_{50,T}$ for sections of the gastrointestinal (GI) tract following ingestion of a radionuclide are discussed below. These sections of the GI tract are treated as separate target tissues (para. 105, *ICRP Publication 26*). Organs and tissues of the body other than the GI tract will also be irradiated by that fraction of the radionuclide which enters the body fluids and also, in some cases, by photon irradiation from material retained in the GI tract. The general methods used to calculate $H_{50,T}$ following entry of a radionuclide into body fluids have been described in Chapter 4. The method used to calculate the activity of an ingested radionuclide or its radioactive daughters, transferred to body fluids from the GI tract, is discussed below.

6.2. Dosimetric Model

The dosimetric model is based on the biological model developed by Eve (1966). For the purposes of radiological protection the GI tract is taken to consist of the 4 sections shown schematically in Fig. 6.1. (See p. 33).

Each of these sections is considered as a single compartment and translocation from one compartment to the next is taken to be governed by first order kinetics. Thus, if $q(t)$ is the activity of ingested radionuclide in a compartment at time t then the model is completely described by the following equations

$$\frac{d}{dt} q_{ST}(t) = -\lambda_{ST} q_{ST}(t) - \lambda_R q_{ST}(t) + \dot{I}(t) \tag{6.1a}$$

$$\frac{d}{dt} q_{SI}(t) = -\lambda_{SI} q_{SI}(t) - \lambda_R q_{SI}(t) - \lambda_B q_{SI}(t) + \lambda_{ST} q_{ST}(t) \tag{6.1b}$$

$$\frac{d}{dt} q_{ULI}(t) = -\lambda_{ULI} q_{ULI}(t) - \lambda_R q_{ULI}(t) + \lambda_{SI} q_{SI}(t) \tag{6.1c}$$

$$\frac{d}{dt} q_{LLI}(t) = -\lambda_{LLI} q_{LLI}(t) - \lambda_R q_{LLI}(t) + \lambda_{ULI} q_{ULI}(t) \tag{6.1d}$$

where λ_R is the radioactive decay constant of the radionuclide in question;

$\lambda_B q_{SI}(t)$ is the rate of transfer of activity to body fluids from the small intestine, assumed to be the only site of absorption from the GI tract to body fluids, and

$\dot{I}(t)$ is the rate of ingestion of activity of the radionuclide at time t.

Similarly, the model for a radioactive daughter produced in the GI tract from its ingested parent radionuclide is completely described by

$$\frac{d}{dt} q'_{ST}(t) = -\lambda_{ST} q'_{ST}(t) - \lambda'_R q'_{ST}(t) + \lambda'_R q_{ST}(t) \tag{6.2a}$$

$$\frac{d}{dt} q'_{SI}(t) = -\lambda_{SI} q'_{SI}(t) - \lambda'_R q'_{SI}(t) - \lambda_B q'_{SI}(t) + \lambda_{ST} q'_{ST}(t) + \lambda'_R q_{SI}(t) \tag{6.2b}$$

$$\frac{d}{dt} q'_{ULI}(t) = -\lambda_{ULI} q'_{ULI}(t) - \lambda'_R q'_{ULI}(t) + \lambda_{SI} q'_{SI}(t) + \lambda'_R q_{ULI}(t) \tag{6.2c}$$

$$\frac{d}{dt} q'_{LLI}(t) = -\lambda_{LLI} q'_{LLI}(t) - \lambda'_R q'_{LLI}(t) + \lambda_{ULI} q'_{ULI}(t) + \lambda'_R q_{LLI}(t) \tag{6.2d}$$

where λ'_R is the radioactive decay constant of the radionuclide in question;

$q'(t)$ is its activity in any compartment and $q(t)$ is the activity of its immediate parent.

The value of λ_B can be estimated from f_1, the fraction of a stable element reaching the body fluids following ingestion:

$$\frac{\lambda_B}{\lambda_{SI} + \lambda_B} = f_1$$

$$\therefore \frac{f_1 \lambda_{SI}}{1 - f_1} = \lambda_B \tag{6.3}$$

Values of f_1 are given in the metabolic data for a number of classes of compounds of each individual element. For radioactive daughters, produced by decay of their parents in the GI tract, the value of f_1 used is usually that appropriate to the stable element of which the ingested radionuclide is an isotope (see Chapter 4). Where a value $f_1 = 1$ is given it is assumed that the radionuclide passes directly from the stomach to body fluids and does not pass through other sections of the gastrointestinal tract.

A system of equations similar to (6.1) and (6.2) can be derived that describe the activities of a chain of parent and daughter radionuclides, the activity of each daughter being determined by the activity of its predecessor in the chain. The metabolic behaviour of all the radioactive progeny is assumed to be the same as that of the ancestral radionuclide which was ingested.

6.3. Activity Transferred from the Respiratory System

The activity of an inhaled radionuclide in any section of the GI tract is described by eqns (6.1a)–(6.1d) in which the term $I(t)$ in eqn (6.1a) is the rate of entry of activity of the radionuclide to the GI tract from the respiratory system (Chapter 5). The activity of a daughter radionuclide in any section of the GI tract is described by eqns (6.2a)–(6.2d) with the addition of a term, $+I'(t)$, to the right hand side of eqn (6.2a). $I'(t)$ is the rate of entry of activity of the daughter radionuclide to the GI tract, the daughter having been produced by decay of its parent in the respiratory system. The value of f_1 for any daughter produced in the respiratory system is usually assumed to be the same as that of the parent radionuclide (Chapter 4).

6.4. Activity Transferred to Body Fluids

The activity transferred to body fluids is the integral over 50 years of $\lambda_B q_{SI}(t)$ for the parent and $\lambda_B q'_{SI}(t)$ for its daughter. Their evaluation is described in the Appendix.

6.5. Calculations of Committed Dose Equivalent, H_{50}, to Sections of the Gastrointestinal Tract

As described in Chapter 4, $H_{50,T}$ for any target organ T from a number of source organs S containing a mixture of radionuclides j is given by

$$H_{50,T} = 1.6\times 10^{-10} \sum_S \sum_j \left[U_S \sum_i \mathrm{SEE}(T \leftarrow S)_i \right]_j \quad \mathrm{Sv} \tag{6.4}$$

where U_S is the total number of transformations in a source organ S over 50 years following intake of a radionuclide j, and

$\mathrm{SEE}(T \leftarrow S)_i$ (in MeV g^{-1} per transformation) is the specific effective energy from radiations of type i originating in S.

When the source organ is a section of the GI tract, U is the integral over 50 years of appropriate values of $q(t)$ from eqn (6.1) and (6.2). Methods of calculating U for a parent radionuclide and its daughters in a section of the GI tract following ingestion of unit activity of the parent radionuclide are discussed further in the Appendix.

$\mathrm{SEE}(T \leftarrow S)_i$, for any radionuclide j, is given by

$$\mathrm{SEE}(T \leftarrow S)_i = \frac{Y_i E_i \mathrm{AF}(T \leftarrow S)_i Q_i}{M_T} \ \mathrm{MeV\ g^{-1}\ per\ transformation}$$

where Y_i is the yield of radiations of type i per transformation of radionuclide j;

E_i (in MeV) is the average, or unique, energy of radiation i;

$\mathrm{AF}(T \leftarrow S)_i$ is the average fraction of energy absorbed in T from radiation i arising in S;

Q_i is the quality factor appropriate for radiation i, and

M_T (in g) is the mass of the target organ.

$H_{50,T}$ is estimated for the walls of each section of the GI tract and it is convenient to consider values of SEE for non-penetrating (np) and penetrating (p) radiations separately. Non-penetrating radiations are, in this context, taken to be heavy recoil particles, fission fragments, α-particles and β-like radiations; penetrating radiations are taken to be x rays, γ rays and fission neutrons.

For both p and np radiations $H_{50,T}$ is calculated for the mucosal layer of each section of the GI tract. For p radiations the average dose to the walls of the tract is used as a measure of the dose to the mucosal layer. Thus, the value of SEE for any target section of the GI tract and for all emissions from radionuclide j within the tract is given by

$$\mathrm{SEE} = \sum_{\mathrm{np}} \frac{Y_{\mathrm{np}} E_{\mathrm{np}} Q_{\mathrm{np}} \mathrm{AF}(\mathrm{ML} \leftarrow T)_{\mathrm{np}}}{M_T^{\mathrm{ML}}} + \sum_S \sum_{\mathrm{p}} \frac{Y_{\mathrm{p}} E_{\mathrm{p}} Q_{\mathrm{p}} \mathrm{AF}(\mathrm{W} \leftarrow S)_{\mathrm{p}}}{M_T^{\mathrm{W}}} \ \mathrm{MeV\ g^{-1}\ per\ transformation}$$

where Y_{np} is the yield of a non-penetrating radiation per transformation of the radionuclide;

E_{np} (in MeV) is the average or unique energy of the non-penetrating radiation;

Q_{np} is 20 for recoil atoms, fission fragments and α-particles and 1 for electrons as described in Chapter 4.

$$\frac{AF(ML \leftarrow T)_{np}}{M_T^{ML}}$$

is the specific absorbed fraction for the mucosal layer of the section of the GI tract under consideration and is taken to be equal to

$$\frac{1}{2} \cdot \frac{1}{M_T^c} \cdot \nu,$$

where M_T^c (in g) is the mass of the contents of that section of the GI tract (Fig. 6.1) and ν is a factor between 0 and 1 representing the degree to which these radiations penetrate the mucus. The factor $\frac{1}{2}$ is introduced because the dose at the surface of the contents will be approximately half that within their volume for np radiations. ν is taken to be unity for β particles, zero for recoil atoms and 0.01 for α particles and fission

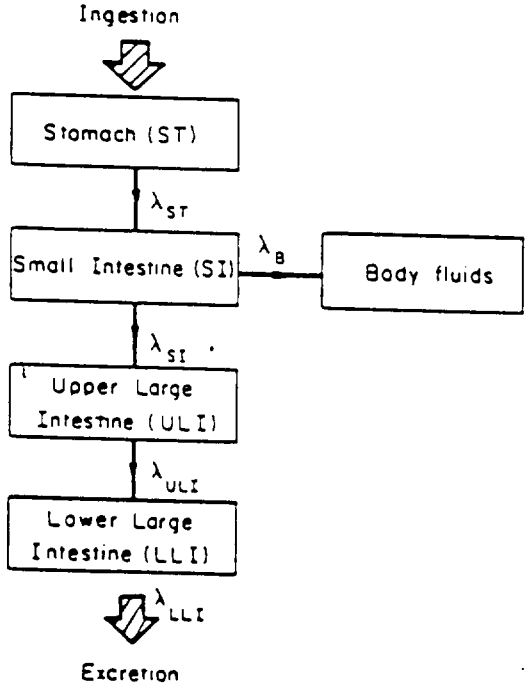

Section of GI tract	Mass of walls* (g)	Mass of contents* (g)	Mean residence time (day)	λ day^{-1}
Stomach (ST)	150	250	1/24	24
Small Intestine (SI)	640	400	4/24	6
Upper Large Intestine (ULI)	210	220	13/24	1.8
Lower Large Intestine (LLI)	160	135	24/24	1

* From *ICRP Publication 23* (1975).

Fig. 6.1. Mathematical model used to describe the kinetics of radionuclides in the gastrointestinal tract

METABOLIC DATA FOR CAESIUM

1. Metabolism

Data from Reference Man (ICRP, 1975).

Caesium content of the body	1.5 mg
of muscle	0.57 mg
of bone	0.16 mg
Daily intake in food and fluids	10 μg

2. Metabolic Model

(a) *Uptake to blood*

Evidence indicates that caesium chloride (LeRoy, *et al.* 1966; Rosoff *et al.*, 1963) and other commonly occurring compounds of caesium (LeRoy *et al.*, 1966) are rapidly and almost completely absorbed from the gastrointestinal tract. In this report f_1 is taken to be unity for all compounds of the element.

(b) *Inhalation classes*

The ICRP Task Group on Lung Dynamics (1966) assigned all compounds of caesium to inhalation class D. The experimental evidence (Miller, 1964; Lie, 1964; Boecker, 1969) is in accord with this classification and it has been adopted here.

Inhalation class	f_1
D	1
W	—
Y	—

(c) *Distribution and retention*

The available evidence indicates that caesium is distributed uniformly in the body. In no case is the concentration of caesium in an organ or tissue of Reference Man (ICRP, 1975) greater than the concentration in muscle.

The retention of caesium is adequately represented over at least the first 1 400 days by a two-exponential expression

$$R(t) = ae^{-0.693t/T_1} + (1 - a)e^{-0.693t/T_2}$$

Values of a have been reported in the range 0.06 to 0.15 (Rundo, 1964), values of T_1 from 1 to 2 days (Rundo, 1964), and values of T_2 from 50 to 150 days with isolated cases up to 200 days (Rundo, 1964; Lloyd *et al.*, 1970; Cryer and Baverstock, 1972; Richmond *et al.*, 1962).

In this report, it is assumed that, of caesium entering the transfer compartment, a fraction, 0.1, is translocated to one tissue compartment and retained there with a half-life of 2 days, whereas the remainder is transferred to a second tissue compartment and retained there with a half-life of 110 days. It is also assumed that caesium translocated to these compartments is uniformly distributed throughout the body.

(d) *Behaviour of daughters*

^{127}Cs decays to ^{127}Xe and, to a small extent, to ^{127m}Xe. ^{127m}Xe, which has a radioactive half-life of 75 s, is assumed to decay at its site of production, whereas ^{127}Xe, with a radioactive half-life of 36 days, is assumed to escape from the body without decaying.

3. Classification of Isotopes for Bone Dosimetry

Caesium is assumed to be uniformly distributed throughout all organs and tissues of the body. Therefore, a classification of isotopes of the element for the purposes of bone dosimetry is not required.

References

Boecker, B. B. (1969). Comparison of ^{137}Cs metabolism in the beagle dog following inhalation and intravenous injection. *Health Phys.* 16, 785–788.

Cryer, M. A. and Baverstock, K. F. (1972). Biological half-life of ^{137}Cs in man. *Health Phys.* 23, 394–395.

ICRP Publication 23, Report of the Task Group on Reference Man. Pergamon Press, Oxford, 1975.

ICRP Task Group Report on Lung Dynamics (1966). Deposition and retention models for internal dosimetry of the human respiratory tract. *Health Phys.* 12, 173–207.

LeRoy, G. V., Rust, J. H. and Hasterlik, R. J. (1966). The consequences of ingestion by man of real and simulated fallout. *Health Phys.* 12, 449–473.

Lie, R. (1964). Deposition and retention of ^{137}Cs in the rat following inhalation of the chloride and the nitrate. *Health Phys.* 10, 1071–1076.

Lloyd, R. D., Mays, C. W., Church, B. W., Pendleton, R. C. and Mays, S. F. (1970). Does the elimination rate of cesium in humans change with the seasons? *Health Phys.* 18, 623–629.

Miller, C. E. (1964). Retention and distribution of ^{137}Cs after accidental inhalation. *Health Phys.* 10, 1065–1070.

Richmond, C. R., Furchner, J. E. and Langham, W. H. (1962). Long-term retention of radiocesium by man. *Health Phys.* 8, 201–205.

Rosoff, B., Cohn, S. H. and Spencer, H. (1963). Cesium-137 metabolism in man. *Radiat. Res.* 19, 643–654.

Rundo, J. (1964). A survey of the metabolism of cesium in man. *Br. J. Radiol.* 37, 108–114.

Annual limits on intake, ALI(Bq) and derived air concentrations, DAC(Bq/m^3) (40 h/wk) for isotopes of caesium

Radionuclide		Oral	Inhalation Class D
		$f_1 = 1$	$f_1 = 1$
^{125}Cs	ALI	2×10^9 (3×10^9) ST Wall	5×10^9
	DAC	—	2×10^6
^{127}Cs	ALI	2×10^9	4×10^9
	DAC	—	1×10^6
^{129}Cs	ALI	9×10^8	1×10^9
	DAC	—	5×10^5
^{130}Cs	ALI	2×10^9 (4×10^9) ST Wall	7×10^9
	DAC	—	3×10^6
^{131}Cs	ALI	8×10^8	1×10^9
	DAC	—	5×10^5
^{132}Cs	ALI	1×10^8	1×10^8
	DAC	—	6×10^4
^{134}Cs	ALI	3×10^6	4×10^6
	DAC	—	2×10^3
^{134m}Cs	ALI	4×10^9 (4×10^9) ST Wall	5×10^9
	DAC	—	2×10^6

METABOLIC DATA FOR PLUTONIUM

1. Metabolism

No data are given in Reference Man (ICRP, 1975) for plutonium. However, there are measurable quantities of the element in foods and in human tissues as a result of world-wide fallout from nuclear weapons tests. There are also data on the distribution of plutonium in people occupationally exposed to the element. These limited human data, in general, support and confirm the much more extensive metabolic data from studies in experimental animals. The metabolism of plutonium, as understood in 1970, was reviewed by an ICRP task group (ICRP, 1972). More recent data have been reviewed in other publications (Dolphin, 1971; Hodge *et al.*, 1973; Bair and Thompson, 1974), notably in the extensive collection of papers in Volume 36 of the Handbook of Experimental Pharmacology (Hodge *et al.*, 1973).

2. Metabolic Model

(a) *Uptake to blood*

Absorption of plutonium from the gastrointestinal tract is low. For f_1 the task group (ICRP, 1972) recommended a value of 3×10^{-5} "for more soluble compounds (e.g. plutonium nitrate)" and a value of 10^{-6} for "relatively insoluble material such as PuO_2 . . .". However, more recent data reviewed by Stather and his co-workers (1979) suggest that higher values of f_1 may be appropriate. In this report f_1 is taken as 10^{-5} for oxides and hydroxides of plutonium and 10^{-4} for all other commonly occurring compounds of the element.

It should be noted that data have been reported which indicate a much higher gastrointestinal absorption for certain compounds of plutonium that are unlikely to be encountered in occupational exposures, e.g. hexavalent plutonium compounds, citrates and other organic complexes; absorption is also increased in the very young (ICRP, 1972).

(b) *Inhalation classes*

The task group (ICRP, 1972) concluded that no plutonium compounds should be assigned to inhalation class D (except chelates, discussed below), that PuO_2 should be assigned to inhalation class Y and that all other commonly occurring compounds of the element should be assigned to inhalation class W. Recent data (Bair *et al.*, 1973; Park *et al.*, 1974; Watts, 1975) have emphasized the complexity of the retention patterns of plutonium compounds in the lung, but do not change the inhalation class assignments. Thus, although $^{238}PuO_2$ is more rapidly translocated from the lung than is $^{239}PuO_2$ and much larger concentrations of ^{238}Pu accumulate in bone and liver (Park *et al.*, 1974), $^{238}PuO_2$ is still best described as a class Y compound.

Inhalation class	f_1
D	—
W	10^{-4}
Y	10^{-5}

(c) *Distribution and retention*

Plutonium absorbed into the blood stream is deposited principally in liver and skeleton. The relative deposition in these two organs has shown a considerable variability in human

619

autopsy, and experimental animal data. The task group (ICRP, 1972) has recommended values of 0.45 for the fractional deposition from blood in liver, 0.45 in bone, and the remaining fraction of 0.10 in all other tissues and early excreta. Based on data from human subjects and from several mammalian species, the task group suggested human biological half-lives of 100 years for retention in the skeleton and 40 years for retention in the liver (ICRP, 1972).

In this report, of plutonium entering the transfer compartment, 0.45 is assumed to be translocated to bone and 0.45 to liver. The data reviewed by Richmond and Thomas (1975) indicate that the fraction of plutonium deposited in the gonads is likely to be about 3×10^{-4} for human males and 10^{-4} for human females. In this report it has been assumed that, of plutonium entering the transfer compartment, the fraction translocated to the gonads is 3.5×10^{-4} for males and 1.1×10^{-4} for females, these values corresponding to a fractional translocation to the gonads of 10^{-5} per g of gonadal tissue in each case. The remainder of plutonium entering the transfer compartment is assumed to go directly to excretion.

Plutonium deposited in gonadal tissue is assumed to be permanently retained there, whereas plutonium deposited in the liver is assumed to be retained with a biological half-life of 40 years and plutonium deposited in the skeleton is assumed to be retained with a biological half-life of 100 years.

(d) *Chelated compounds*

Chelated forms of plutonium are not considered in this report. It is known that they move to some extent across the gut wall but also that they are more readily excreted than are other compounds of plutonium (Baxter and Sullivan, 1972).

3. Classification of Isotopes for Bone Dosimetry

Plutonium mainly deposits upon the endosteal surfaces of mineral bone and is slowly redistributed throughout its volume by processes such as resorption and burial (Vaughan, 1973; Schlenker *et al.*, 1976). For this reason all isotopes of plutonium considered in this report are assumed, for the purposes of dosimetry, to be uniformly distributed over bone surfaces at all times following their deposition in the skeleton.

References

Bair, W. J. and Thompson, R. C. (1974). Plutonium: biomedical research. *Science* 183, 715–722.

Bair, W. J., Ballou, J. E., Park, J. F. and Sanders, C. L. Plutonium in soft tissues with emphasis on the respiratory tract. In: *Uranium, Plutonium, Transplutonium Elements*, Eds, Hodge, H. C., Stannard, J. N. and Hursh, J. B., pp. 503–568. Springer-Verlag, Berlin, 1973.

Baxter, D. W. and Sullivan, M. F. (1972). Gastrointestinal absorption and retention of plutonium chelates. *Health Phys.* 22, 785–786.

Dolphin, G. W. (1971). The biological problems in the radiological protection of workers exposed to ^{239}Pu. *Health Phys.* 20, 549–557.

Hodge, H. C., Stannard, J. N. and Hursh, J. B., Eds. *Uranium, Plutonium, Transplutonium Elements* (Handbook of Experimental Pharmacology, Vol. 36). Springer-Verlag, Berlin, 1973.

ICRP Publication 19, The Metabolism of Compounds of Plutonium and Other Actinides. Pergamon Press, Oxford, 1972.

ICRP Publication 23, Report of the Task Group on Reference Man. Pergamon Press, Oxford, 1975.

Park, J. F., Catt, D. L., Craig, K. D., Olson, R. J. and Smith, V. H. Solubility changes of ^{238}Pu oxides in water suspension and effect on biological behaviour after inhalation by beagle dogs. In: *Proc. Third Int. Cong. Int. Radiat. Prot. Assn., Washington DC September 1973*, Ed. Snyder, W. S., Vol. 1, pp. 719–724 (CONF-730901-P1), 1974.

Richmond, C. R. and Thomas, R. L. (1975). Plutonium and other actinide elements in gonadal tissue of man and animals. *Health Phys.* 29, 241–250.

6. Assume that ^{239}Pu gives off a 5-MeV alpha particle per decay and that its half-life is 24,000 years.
   a. Use the attached metabolic data for plutonium and the ICRP-30 model to calculate the total number of transformations occurring over 50 years in the liver, bone, and gonad for an ingestion of 1 Bq of $^{239}PuO_2$.
   b. If the intake route of the 1 Bq of $^{239}PuO_2$ (1 μm AMD) is inhalation, what is the consequence? Would it be better or worse (from cancer risk viewpoint) compared to the ingestion case? Why?